THE EFFECT OF HYDROFLAPS ON THE PITCHING AND BRAKING OF FLYING BOATS

THEODORE FEUERBACH

DIRECTIONS FOR BINDING

BIND IN
(CIRCLE ONE)

BUCKRAM
COLOR NO. 8854

FABRIKOID
COLOR_____

LEATHER
COLOR_____

OTHER INSTRUCTIONS
Letter in gold.

LETTERING ON BACK TO BE EXACTLY AS PRINTED HERE.

shelf

FEUERBACH

1951

THESIS
F27
c.1

• Letter on the front cover:

THE EFFECT OF HYDROFLAPS
ON THE PITCHING AND BRAKING OF
FLYING BOATS

THEODORE FEUERBACH

THE EFFECT OF HYDROFLAPS ON THE PITCHING AND BRAKING OF FLYING BOATS

A Thesis Submitted in Partial Fulfillment
of the Requirements for the Degree of
Master of Science

STEVENS INSTITUTE OF TECHNOLOGY

Submitted by Theodore Feuerbach

TABLE OF CONTENTS

SUMMARY

This investigation was made to determine, by means of towing tank tests, the effect of hydroflaps on the pitching and braking of flying boats. The effect of hydroflaps on steering is covered in a previous report by Beck.

An analysis of the pitching moment was made by comparing the analytical solution with the towing tank test results of a model hull. The analytical equation was derived for the purpose of predicting the general effect of opening one or two hydroflaps on the moments of flying boats. The parameters used were flap-opening angle (α), hinge angle (θ), deadrise angle (β), and moment arm. The effect of various parameters when substituted in the moment equation followed a general pattern similar to the experimental curves.

The effect of a change in deadrise was not observed experimentally because only one model was tested, but as noted in the solution of the analytical equation, an increase in deadrise caused a decrease in negative moment. At small hinge angles and large flap-opening angles, the moments reversed from negative (hull nose down) to positive (hull nose up).

The resistance of the model hull steadily increased when both flaps were extended from a closed position ($\alpha = 0^{\circ}$) to a fully-opened position ($\alpha = 90^{\circ}$). An increase in hinge angle from 47° to 59° produced an increase in resistance for all flap openings over 40°.

As the flap-opening angle and hinge angle were increased, it was found that the percent saving in time and landing-run distance of the hull alone as compared to several modifications on the hull increased to 32% and 38%, respectively.

This investigation was conducted at the Experimental Towing Tank, Stevens Institute of Technology, Hoboken, N.J.

INTRODUCTION

The present investigation was conducted to study the effects of hydroflaps on flying boats and, if possible, to correlate the analytical data and the experimental test data of the forces acting on hydroflaps. The experimental work was the combined efforts of Beck (Reference 1) and the writer. The object of Beck's work was to investigate the effect of hydroflaps on steering ability, while the present report is concerned with the pitching moments and braking action resulting from the use of hydroflaps.

In the past ten years the design of flying boats has changed because of the increased power requirements, the favorable stability characteristics of long afterbodies, and the desire for greater payload capacity. The development of present seaplanes and flying boats has reached a stage where greater emphasis must be placed upon the maneuverability of such hulls after the landing run and in taxiing.

Up to this period, flying boats were underpowered, in comparison with present-day standards, and had slower taxiing speeds under idling conditions. The short afterbodies are now gradually being replaced by longer afterbodies in an effort to reduce the impact loading caused by the increased weight requirements and the increasing requirements for rough-water operations. A great deal of research and development on the shape of flying-boat hulls (Reference 2) indicated the need of im-

proved devices for directional control and braking, and has resulted in certain developments of such devices for slow maneuvering on water and in the ability to make quick stops while taxiing (References 3,4).

Devices such as the water rudder are common to small seaplanes (Reference 5), while the sea anchor, common to most military seaplanes, is thrown overboard and controlled by crew members who have to pay out or pull in line, as directed by the pilot, to produce the necessary drag. This method is awkward to handle and at times not available at the instant required to prevent accidents.

Extensive work has been conducted at the Experimental Towing Tank, Stevens Institute of Technology, on various hull appendages designed to reduce the turning circle and for braking action. These appendages include hydroflaps, spoilers, rudders, water scoops, and step-fairing flaps. With the introduction of reverse pitch propellers on large flying boats, the braking action was most successful, but under adverse conditions of high winds and small maneuvering area, the short delay of changing pitch still remained a problem to pilots.

The PBM-1 Martin Marlin (Reference 3) has flaps installed on the afterbody bottom near the stern which are capable of opening to 65° to the bottom. These flaps serve the same purpose for braking as the dive flaps on military divebombers. They are controlled by the pilot from the cockpit and can be opened

individually or as a pair, whichever is necessary for turning or braking. The flap has reduced the turning radius by at least 50% over old-style seaplanes. The flaps referred to in Reference 3 are now known as hydroflaps.

The present investigation is concerned with the effect of hydroflaps on the pitching moment and braking action of flying boats. The test data collected covered the effects of yaw (investigated by Beck, Reference 1) and trim under the parameters of hinge angle (θ) with the afterbottom keel, and flap-opening angle (α) for the flap installed, either singly or on both sides of the afterbody bottom for trim and on both sides for braking.

The tests were limited to the study of only one seaplane hull model (Figure 2) with a constant deadrise angle (β) of 20°, and three model test speeds -- in coefficient form, $C_{V_1} = 1.06$, $C_{V_2} = 1.54$, and $C_{V_3} = 2.02$ -- in the range below hump speed.

Three sets of hydroflaps, each with a different hinge angle of 21°, 47°, and 59° (Figure 3), were tested with modifications of the angle between the hydroflap and the afterbody bottom of 30°, 60°, and 90° (Figure 4).

This investigation was conducted at the Experimental Towing Tank, Stevens Institute of Technology, Hoboken, N.J., under the guidance of Professor B.V. Korvin-Kroukovsky, whose advice has proved invaluable in the compilation of this thesis.

SYMBOLS AND NOTATIONS

Load coefficient	C_Δ	$= \Delta/wb^3$
Lift coefficient	C_L	$= L/\frac{1}{2}\rho V^2 S$
Trimming moment coefficient	C_M	$= M/\frac{1}{2}\rho V^2 AL$
Yawing moment coefficient	C_{M_ψ}	$= M_\psi/wb^4$
Resistance coefficient	C_R	$= R/wb^3$
Speed coefficient	C_V	$= V/\sqrt{gb}$

A = Area of hydroflap

b = Maximum beam, ft.

C = Coefficient

g = Acceleration due to gravity (32.2 ft./sec.^{2})

L = Lift, or weight of plane, lb.

M = Trimming moment, in.lb. (water moments tending to raise bow considered positive)

M_ψ = Yawing moment, in.lb.

R = Water force along longitudinal axis of hull, lb.

S = Wing area, ft.^{2}

V = Speed, ft./sec.

w = Specific weight of water (62.3 lb./ft.^{3})

α = Angle between flap and afterbody bottom, deg.

β = Angle of deadrise, deg.

Δ = Waterborne load, lb.

η_m = Maximum efficiency

θ = Angle between keel line and hinge line of flap, deg.

λ = Ratio of model to full-scale dimensions

ρ = Density

γ = Trim angle, deg.

Ψ = Yaw angle, deg.

MATERIAL AND APPARATUS

Description of Hydroflaps

Hydroflaps for use on seaplanes and flying boats are similar to the split flaps on wings which are called dive flaps, or to the flaps on each side of the fuselage of military divebombing planes, and when opened, serve the same purpose for braking. In addition to their use as a brake, hydroflaps may be opened singly for steering.

Hydroflaps are installed on the afterbody bottom in the vicinity of the stern and are controlled by the pilot in the cockpit. In order to reduce unnecessary drag, the flaps are recessed into the hull bottom where the flap angle (α) is zero, and then opened to the desired flap angle with the afterbody bottom.

The shape and size of the hydroflaps depend on the shape of the afterbody bottom, installation point, weight of plane, and taxiing speeds. The hydroflaps used for this investigation were designed to be similar to the spoilers used in Reference 3, and were cut from 0.031-in. sheet brass (see Figure 3).

Three sets of hydroflaps were made with the aspect ratio held constant, and the area of each equal to 1.5 sq.in. They were different only in the amount of hinge angle (θ), which was one of the parameters of this investigation. The angle (α) between the flap and the afterbody bottom of the model was formed by using the same flap for all α's. The desired angle of open-

ing for each test was obtained by removing the flap from the model, bending it along the hinge line to $\alpha = 30^{\circ}$, 60°, or 90°, and then replacing the flaps on the model.

Description of Model

A 1/8-scale hull model of a hypothetical flying boat was used for this investigation. Drawings of the body plan are shown in Figure 2. This model was one of a series of hulls previously tested at the Experimental Towing Tank, Stevens Institute of Technology, to determine its suitability for small flying boats (Reference 6), and can be considered as a typical long-afterbody hull.

A forebody hull (E.T.T. Model No. 1043) was attached to an afterbody section (E.T.T. Model No. 1055-01) (Reference 6) to give a complete model hull with a long afterbody, which seems to be the design trend on present-day flying boats. The dimensions of the model and full-scale flying boat are as follows:

Main Dimensions of Hypothetical Seaplane

	Full Scale*	Model
Scale	1	1/8
Gross weight, lb.	2900	
Forebody length, in. (Model No. 1043)	156	19.5
Afterbody length, in. (Model No. 1055)	216	27

* The actual size visualized in Reference 6 is not relevant to the present investigation since the hull shape is merely considered as typical for the long-afterbody form and the test results and analytical data expressed in nondimensional form.

	Full Scale	Model
Beam, in.	42	5.25
Deadrise at step, deg.	20	20
Step height, in.	4	0.5
Sternpost angle, deg.	8	8
C.G. location forward of step, in.	12.0	1.5
C.G. location above forebody keel, in.	52.0	6.5
Wing area, sq.ft.	272	
Horsepower	185	
Coefficient of lift (take-off)	1.2	

Ratios: $\frac{\text{Full Scale}}{\text{Model}}$

Speed	$\lambda^{\frac{1}{2}} = 2.81$
Length	$\lambda = 8.00$
Area	$\lambda^2 = 64$
Volume	$\lambda^3 = 512$
Moment	$\lambda^4 = 4096$

Towing Tank

All tests were conducted in Tank No. 1 of the Experimental Towing Tank, Stevens Institute of Technology; the tank is 95 ft. long and has a semi-circular cross-section $4\frac{1}{2}$ ft. in radius. An additional 6-ft. section of smaller cross-section is located at one end for the convenience of work in mounting the test model to the carriage. The carriage runs on a single rail suspended over the centerline of the length of the tank and receives its

motion by being connected to a towing line which is driven by a multiple diameter cone pulley. The carriage speeds may be varied by means of exchangeable gear boxes, and the cone pulley may be varied from 1 to 30.8 ft./sec. as desired. The power for operating the carriage is supplied by direct current to bring the model up to speed. Then an A.C. synchronous motor cuts in to operate the carriage at constant speed.

Apparatus

The apparatus for the pitching and yawing tests was designed by the E.T.T., S.I.T. (References 5,7), and is shown in Figure 5. The main towing gate was connected to the carriage while the other parts (Figures 5 through 8) were either fixed to the towing gate or moved on pivots fixed to the towing gate.

A vertical shaft, which contained a yoke with pivot points to which was attached the model on bearings located at its center-of-gravity position (6.5 in. above forward keel line and 1.5 in. forward of step), allowed the model freedom in pitch and yaw as shown in Figure 8. The angular motion of the vertical shaft attached to the model was restrained by a calibrated spring for the determination of the yawing moment. A dashpot allowed for damping in yaw.

For the resistance tests, a dynamometer was connected to the forward part of the carriage as shown in Figure 9. This apparatus was comprised of a bell crank lever, with one end of the lever attached to the towing bar of the main gate and the other

end to a weight pan for recording the resistance of the model. A dashpot was installed to reduce the oscillation of the lever. Forward of the bell crank lever was a sensitive calibrated spring with a scale and pointer attached to the towing bar. The readings on the scale were additive to the pan weight in determining the total resistance of the model.

Wind resistance at the speeds used for this investigation was found to be negligible from previous tests (Reference 6) and was therefore neglected.

METHODS AND PROCEDURE

For this investigation, a flying-boat forebody (E.T.T. Model No. 1043) was connected to an afterbody (E.T.T. Model No. 1055), and then the complete model was modified as follows: A set of pivot points was installed at the center of gravity; a trim scale was installed on the afterbody; and weight masts were erected fore and aft for balancing the model about the center-of-gravity point.

After the model was balanced, it was connected to the towing carriage at the pivot points, and weights were added to the main towing gate in accordance with the values of load required for the speed coefficients of C_V = 1.06, 1.54, and 2.02. The loads for the various speeds, shown on page 27, were obtained from the results of a parabolic unloading curve (Reference 8) based on a full-scale weight of 2900 lb., a wing area of 272 sq.ft., 185 horsepower, and a lift coefficient $(C_L)_{take\text{-}off}$ of 1.2.

Since the object of this investigation was to find the change in the trim for the change of flap, it was desirable to show trim $(\tau)^*$ in terms of moments. To obtain a reference point and to establish a relation between trim and the moment applied to it, a series of tests was run with weights added to the forward and after weight masts on the model. The results

---

* τ is the vertical angle formed by the horizontal plane and the straight portion of the forebody keel at the step.

are shown in Figure 10 for three speeds, C_V = 1.06, 1.54, and 2.02, and three angles of yaw (ψ), 5° port, 0°, and 5° starboard.

The procedure for each test was essentially the same. A flap was installed on one side of the afterbody bottom for the yawing tests, on one or two sides for the pitching tests, and on both sides for the braking tests.

The modifications on the bare hull model were as follows:

1. Flaps added; $\alpha = 0°$
2. Port flap added; $\theta = 21°$; $\alpha = 30°$, 60°, and 90°
3. Port flap added; $\theta = 47°$; $\alpha = 30°$, 60°, and 90°
4. Port flap added; $\theta = 59°$; $\alpha = 30°$, 60°, and 90°
5. Both flaps added; $\theta = 21°$; $\alpha = 30°$, 60°, and 90°
6. Both flaps added; $\theta = 47°$; $\alpha = 30°$, 60°, and 90°
7. Both flaps added; $\theta = 59°$; $\alpha = 30°$, 60°, and 90°

For the resistance tests, the dynamometer (Figure 9) was connected to the towing arm and carriage, and the spring calibrated. The resistance characteristics of the bare hull were recorded as a comparison with the modified model. Only two speeds were used: C_V = 1.06 and 2.02. The modified model tests were conducted with both flaps, $\theta = 47°$ and 59°, and $\alpha = 30°$, 60°, and 90°.

RESULTS

The trim and yaw data obtained from the towing tank investigation of the hypothetical seaplane model (E.T.T. Model No. 1043, 1055) are presented in graphical form in Figures 11 through 19 as trim (τ) vs. yaw (ψ), with the parameters of speed, hinge angle (θ), flap-opening angle (α), and either single or double flap installed. They are also presented in tabular form in Table Ia-o.

Figure 10, which is a calibration curve necessary for the reduction of the experimental data, shows the applied pitching moment vs. trim angle, which is also tabulated in Table II. The data were obtained by applying various loads at either the forward or after weight masts (Figure 5), towing the model down the tank, and recording the trim. During all runs, the yaw angle (ψ) was locked at the angle desired.

Figure 20 is a plot of resistance (R) vs. velocity (V). The resistance data are also tabulated in Table III. The effective thrust line data were obtained from the section FORMULAE AND ANALYTICAL ANALYSIS. Two curves, $\alpha = 70^{\circ}$ and $\theta = 35^{\circ}$, 47°, were interpolated.

Figure 21 is a plot of R/V^2 vs. α for the two hinge angles (θ) of 47° and 59°. The data were taken from Figure 20.

The pitching moment characteristics of the model with modifications of flap are recorded in Figures 22 through 27 as moment coefficient (C_M) vs. flap-opening angle (α). A compari-

son of the experimental results and the analytical results is also shown in the above curves. The data necessary for the analytical curves may be found under FORMULAE AND ANALYTICAL ANALYSIS, and in Table IV. The curves represent the effect of moment due to flap, since they were taken as the difference between the readings of hull alone and of hull plus flap.

Figures 28 and 29 are plots of C_M vs. α. The data for the curves, tabulated in Table IV, were computed by substituting $\beta = 20^\circ$ and 40° in the analytical equation derived on page 26.

Figure 30 is a cross plot of values taken from Figure 20, presented in the form of $1/F$ vs. V, and V/F vs. V, where F is the total retarding force.

DISCUSSION

The experimental model under investigation for this series of tests was found to be slightly unstable in the clean state. With the addition of hydroflaps, however, the stability was favorably increased to the extent of reaching neutral stability in the range of flap angles tested (Reference 1).

The trim (τ) vs. yaw (ψ) curves obtained (Figures 11 through 19) show only a small deviation from a straight line for the range of yaw angles tested. At $C_V = 1.06$, the change in trim (τ) of the hull alone as compared to the hull plus hydroflaps at various settings was negligible. At higher speeds, $C_V = 1.54$ and $C_V = 2.02$, the trim changed slightly when one flap was opened, and further increased when both flaps were extended.

It was expected that in all cases the opening of the flaps would tend to give a negative moment (nose-down attitude), but under investigation it was observed that at low hinge angles (θ), the hull had positive moments at $C_V = 1.54$ and $C_V = 2.02$ and flap settings (α) = 60° and 90° (Figures 12 and 13). A visual check of the flap on several model hulls, at the various parameters of hinge angle (θ), flap-opening angle (α), and deadrise angle (β), clearly showed that the flow of water on the outward face of the flap gave a positive moment (nose-up) under certain conditions of flap settings: when the hinge angle (θ) was in the range of 20° and below, and at large openings of the

flap. An increase of deadrise angle (β), with all other parameters held constant, would have the effect of increasing the moment in the positive direction (nose-up). This observation was verified in the static pitching moment curves (Figures 28 and 29) which were based on an analytical equation using the parameters of β, θ, and α.

The pitching moment equation on page 26 was derived with the assumption that only the forces acting on the flaps were considered. The experimental data represent the total moment due to the force on the flaps and on the adjacent parts of the hull. Under experimental conditions using one flap, the flow of water was observed to form a spray aft of the flap and, at all times, the afterbody was completely supported by water in the range of speeds tested. With two flaps installed, one on each side of the afterbody bottom, the sternpost was completely clear of the water (Figures 6 and 7). Directly aft of the flaps (inner surface), there was an air space, with the flow of water along the keel forming a roach after passing the opened flaps and striking the hull bottom. To include experimental data on the above observation would necessitate recording the actual flow pattern and the forces acting on the flaps, making a study of spray and roaching characteristics, and taking underwater photographs, in addition to making a study of several model hulls with variation in deadrise angle (β) -- all of which was beyond the scope of this study in material and time.

Beck (Reference 1) found that, as far as maneuverability is concerned, there was an optimum value of flap opening, i.e., $\alpha = 70^{\circ}$, and upon further opening, little improvement was realized. As far as braking is concerned (Figure 20), there was a steady increase in braking power with an increase in flap opening, with no limit of resistance observed. With regard to hinge angle (θ), Beck observed that the yawing moments decreased greatly beyond $\theta = 40^{\circ}$, although the reason was not determined. Within the range of flap openings tested ($\alpha = 30^{\circ}$ to 90°), braking was improved by increasing the hinge angle ($\theta = 47^{\circ}$ to 59°) (Figure 21).

The expression $T = \frac{W}{g}\int \frac{1}{F} dV$, taken from Reference 9, was used to determine percent saving in time of the landing run. (Here, F = total retarding force, lb.; V = model speed, ft./sec.; W = gross weight of model, lb.; g = acceleration due to gravity; and T = time, sec.) The solution was obtained by plotting 1/F vs. V (Figure 30). The landing-run distance was obtained in a similar manner by using the expression $S = \frac{W}{g}\int \frac{V}{F} dV$, also taken from Reference 9, plotted as V/F vs. V in Figure 30. (Here, S = distance, ft.) The results are tabulated below:

Modification		Time, %	Landing-Run Distance, %
Flap-Opening Angle, deg. (α)	Hinge Angle, deg. (θ)		
90	59	32	38
70	47	20	26
70	35	15	15

Figures 22 through 27 show a comparison of the analytical solution with the experimental results in the nondimensional form C_M vs. α. The experimental curves seem to follow a general pattern, deviating slightly from the analytical curves. The analytical derivation of the moment equation, in addition to the pitching moment components, contained the yawing moment which has been verified by Beck (Reference 1), and found to be satisfactory in the comparison of experimental data with the analytical analysis.

It is expected that in the actual installation of hydroflaps on flying boats, the flap will be installed flush with the afterbody bottom, with the thickness of the flap extending into the hull. Upon opening the flaps, the flow of water between the flaps along the keel may roach, thus striking the actuating rods and structure located in the flap housing, and causing a slight change in trim from the results observed in these tests. In all cases it is believed that the effect of pitching will not be critical and may be corrected easily by proper application of controls by the pilot.

FORMULAE AND ANALYTICAL ANALYSIS

Analytical Method of Determining the Force Component on the Hydroflap

In the derivation of the equation of static pitching moment, the major parameters were hinge angle (θ), flap-opening angle (α), and deadrise angle (β). The analysis is based on the following assumptions:

1. Only the force of water pressure on the flap is determined. The forces acting on the hull itself are subsequently established as a comparison with the experimental results and the flap forces.
2. The model is towed at low speeds comparable to taxiing speeds, with the hydroflap submerged at all times.
3. The flow of water is parallel to the afterbody keel.
4. The application of the force vector is located at the intersection of the hinge line and afterbody keel. The difference of the actual point of application and the assumed point is small as compared to the moment arm from the center of gravity of the model to the point on the keel used.

The geometry of the afterbody with the angles α, β, and θ is shown in Figures 4 and 31. The axes X,Y,Z are as indicated, with the X axis along the afterbody-keel line, positive toward bow, right-handed system. Line F O is the hinge line; the

plane ABCD is on one side of the afterbody bottom; O is the origin of the X,Y,Z axes; and the X Z axes is the plane of symmetry.

Geometrical Relations: The normal form of the equation for a plane is (Reference 10):

$$X \cos a + Y \cos b + Z \cos c - P = 0, \qquad (1)$$

where P is the perpendicular distance from the origin to the plane, and a, b, and c are the direction cosines of that perpendicular. The plane of the afterbody bottom ABCD is:

through the origin at O $\therefore P = 0$,

through the X axis $\therefore a = 90^{\circ}$ and $\cos a = 0$,

$\cos b = \cos (90 - \beta) = \sin \beta$,

$\cos c = \cos \beta$.

Substituting the above values into equation (1) gives:

$$0 + Y \sin \beta + Z \cos \beta = 0$$

$$Z = -Y \tan \beta . \qquad (2)$$

The equation of a plane passing through the hinge line OF (Figure 31) in terms of the parameters β and θ is:

$$FE = \frac{Z}{\sin \beta} \quad \text{and also} \quad FE = -X \tan \theta$$

$$\therefore \quad \frac{Z}{\sin \beta} = -X \tan \theta$$

or

$$Z \csc \beta + X \tan \theta = 0 . \qquad (3)$$

The equation of a plane which satisfies two conditions

will, in general, contain an arbitrary constant. The system of planes passing through the line of intersection of two given planes is represented by:

$$A_1X + B_1Y + C_1Z + D_1 + K(A_2X + B_2Y + C_2Z + D_2) = 0 ,$$

where K is the arbitrary constant (Reference 10). Combining equations (2) and (3) gives the equation of a system of planes passing through the hinge line:

$$Z \csc \beta + X \tan \theta + K(Z + Y \tan \beta) = 0$$

$$(\tan \theta)X + (K \tan \beta)Y + (\csc \beta + K)Z = 0 . \qquad (4)$$

The direction numbers of the equation for the afterbody bottom (2) and the system of planes passing through the hinge line are:

(0, tan θ, 1) (from equation (2))

(tan θ, K tan β, K + csc β) (from equation (4)) .

In order to find the flap-opening angle (α), or the angle between the planes shown by equations (2) and (4) (Reference 10), the following equation is used:

$$\cos \alpha = \frac{A_1A_2 + B_1B_2 + C_1C_2}{\pm\sqrt{A_1^2 + B_1^2 + C_1^2}\ \pm\sqrt{A_2^2 + B_2^2 + C_2^2}}$$

or

$$\cos \alpha = \frac{0 + K \tan^2 \beta + K + \csc \beta}{\sqrt{\tan^2 \beta + 1}\ \sqrt{\tan^2 \theta + K^2 \tan^2 \beta + (K + \csc \beta)^2}} \qquad (5)$$

For actual test conditions, the various parameters α, β, and θ will be known. Therefore, the only unknown is K. By squaring both sides of the above equation, a quadratic equation in terms of K is obtained:

$$K^2(\sin^2\alpha \sec^4\beta) + K(2 \csc\beta \sec^2\beta \sin^2\alpha) + \sin^2\alpha(\csc\beta - \cot\alpha \sec^2\beta \sec^2\theta) = 0 .$$

Dividing the above equation by $\sin^2\alpha \sec^4\beta$ and solving for K by the quadratic formula gives:

$$K = -\csc\beta \cos^2\beta - \cot\alpha \cos\beta \sec\theta .$$

The equation of the normal of the system of planes through the hinge line is also the equation of the line containing the force vector on the hydroflap. From previous assumptions, the force vector was applied at the intersection of the hinge line and the afterbody keel (0,0,0). The equation for the line perpendicular to the system of planes therefore becomes:

$$\frac{X}{\tan\theta} = \frac{Y}{K \tan\beta} = \frac{Z}{\csc\beta + K} .$$

The equation of a plane (4) is reduced to the normal form by dividing by:

$$\sqrt{(\tan\theta)^2 + (K \tan\beta)^2 + (\csc\beta + K)^2}$$ (Ref.10,p.253)

Substituting the value of K in the above radical gives:

$$\left[\tan^2\theta + (-\csc\beta \cos^2\beta \tan\beta - \cot\alpha \cos\beta \sec\theta \tan\beta)^2 + (\csc\beta - \csc\beta \cos^2\beta - \cot\alpha \cos\beta \sec\theta)^2\right]^{\frac{1}{2}} .$$

Reducing and combining terms gives:

$$\left[\tan^2\theta + (-\cos\beta - \cot\alpha \sec\theta \sin\beta)^2 + (\sin\beta - \cot\alpha \cos\beta \sec\theta)^2\right]^{\frac{1}{2}}$$

$$= \left[\tan^2\theta + 1 + \cot^2\alpha \sec^2\theta\right]^{\frac{1}{2}} = \left[\sec^2\theta(1 + \cot^2\alpha)\right]^{\frac{1}{2}}$$

$$= \sqrt{\sec^2\theta \csc^2\alpha} = \sec\theta \csc\alpha \quad .$$

The equation of the plane normal to the system of planes, equation (4), is found by dividing by (sec θ csc α):

$$\left(\frac{\tan\theta}{\sec\theta \csc\alpha}\right)X + \left(\frac{-\cos\beta - \cot\alpha \sec\theta \sin\beta}{\sec\theta \csc\alpha}\right)Y + \left(\frac{\sin\beta - \cot\alpha \cos\beta \sec\theta}{\sec\theta \csc\alpha}\right)Z = 0 \quad .$$

Reducing the above equation gives:

$$(\sin\theta \sin\alpha)X + (-\cos\beta \sin\alpha \cos\theta - \cos\alpha \sin\beta)Y + (\sin\beta \cos\theta \sin\alpha - \cos\alpha \cos\beta)Z = 0 \quad .$$

Since the flow was assumed parallel to the keel line, the correction angle $\bar{\alpha}$ was found as follows: The perpendicular distance from a point on the keel (-1, 0, 0) to the plane of the hydroflap was found by substituting the values of the point into the equation $X \cos a + Y \cos b + Z \cos c = D$, where D is the perpendicular distance and the equation is in the normal form (Reference 10, p. 263):

$$D = -\sin\theta \sin\alpha$$

$$\sin\bar{\alpha} = \frac{D}{X} = \frac{-\sin\theta \sin\alpha}{-1} = \sin\theta \sin\alpha \qquad \text{(Figure 31)} \quad .$$

The final moment equation becomes:

$$M = \frac{\rho}{2} AV^2 \sin \bar{\alpha} \Big[L_2(\sin \theta \sin \alpha) + L_1(-\cos \beta \sin \alpha \cos \theta - \cos \alpha \sin \beta) + L_1(\sin \beta \cos \theta \sin \alpha - \cos \alpha \cos \beta) \Big] .$$

For pitching only, the X and Z components were considered. Reference 1 covers the Y components affecting yaw. The final equation in coefficient form is:

$$C_M = \frac{M}{\frac{\rho}{2} AV^2 L_1} = \left[\frac{L_2}{L_1} (\sin \theta \sin \alpha)^2 + (\sin \theta \sin \alpha)(\sin \beta \cos \theta \sin \alpha - \cos \alpha \cos \beta) \right].$$

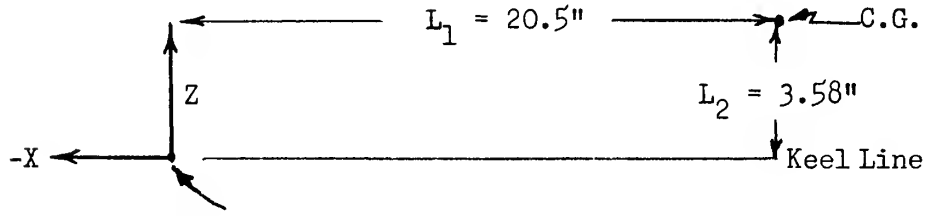

Intersection of hinge line with keel.

Formulae and Sample Calculations

For the parabolic unloading curve:

$$\Delta_o = \tfrac{1}{2} \rho V_o^2 S C_L$$

$$V_o^2 = \frac{2\Delta_o}{\rho S C_L} = 7500,$$

where Δ_o = 2900 lb.

S = 272 sq.ft.

C_L = 1.2

λ = 8 .

Therefore,

$$V_o = 86.5 \text{ ft./sec.} \quad ,$$

and from Reference 8.

$$\Delta_m = \frac{\Delta_o}{(8)^3}\left[1 - \left(\frac{V}{V_o}\right)^2\right] .$$

Substituting the values of V_o and V, and changing to coefficient form, where $C_V = V/\sqrt{gb}$ and $C_\Delta = \Delta/wb^3$, give the following values:

V	C_V	C_Δ
3.98	1.06	1.085
5.76	1.54	1.045
7.56	2.02	0.99

The thrust line in the resistance curve (Figure 20) was found as follows:

Assume maximum speed of aircraft at 120 miles/hr.

$\lambda = 8$

$\lambda^{\frac{1}{2}} = 2.83$

$V_{\text{max. model}} = 62.2 \text{ ft./sec.}$

Maximum RPM = 2250

Idling RPM = 500

$$EHP = \frac{RV}{550} = \frac{1.08 \times 7.5}{550} = 0.0147$$

$$R = \frac{0.0147 \times 550}{V_m}$$

$$V/nd = \frac{V_m}{62.2}\,\frac{2250}{500} = 0.0725\ V_m$$

The results obtained are:

V_m	R	V/nd	η_m	Ratio	Thrust
7.5	1.08	0.545	0.76	1.00	1.08
7.0	1.16	0.508	0.75	0.987	1.14
6.5	1.25	0.471	0.73	0.96	1.20
6.0	1.35	0.435	0.71	0.935	1.26
5.5	1.47	0.400	0.69	0.91	1.34

The curve V/nd vs. η_m is found in Reference 11.

CONCLUSIONS

The pitching moment equation derived in this investigation is:

$$M = \tfrac{1}{2} \rho V^2 \sin \bar{\alpha} \left[L_2(\sin \theta \sin \alpha) + L_1(\sin \beta \cos \theta \sin \alpha - \cos \alpha \cos \beta) \right] .$$

This analytical expression was computed by considering only the forces acting on the flap, while the experimental work takes into account the total moment due to the forces acting on the flap and on the adjacent parts of the hull (see Figures 22 through 27). The general trend of the curves compared favorably and indicated the probability of the pitching moment to increase and reach a maximum in a negative manner upon extending the flaps (in the range of $\alpha = 40^\circ$). When the flaps were opened further, the negative moment decreased, reaching a positive nose-up attitude. This reversal occurred at low settings of hinge angle ($\theta = 20^\circ$) and large openings of the flap ($\alpha = 70^\circ$).

Since only one model was tested, a check on the effect of deadrise angle (β) in pitching was not observed experimentally, although a solution of the pitching moment equation indicates that an increase in deadrise angle, with all other parameters held constant, would effectively reduce the negative moment in the range of flap openings up to $\alpha = 70^\circ$.

The braking power was increased with an increase in flap opening, and also by enlarging the hinge angle. With flaps ex-

tended to 90° and a hinge angle of 59°, the reduction in landing time and landing run was 32% and 38%, respectively. The effect of the change in deadrise was not observed because only one model was tested.

In determining the maximum setting of hinge angle and flap opening, a comparison of the relative value of maneuverability and braking should be made. Maneuverability is more important than braking when considering the great need for control in making a buoy and correcting for cross-winds. Beck (Reference 1) stated that the optimum value of flap opening and hinge angle was around 70° and 35°, respectively. For these conditions, the saving in the landing run would be approximately 15%.

REFERENCES

1. Beck, P. Investigation of Hydroflaps for Steering Seaplanes. Thesis at Stevens Institute of Technology, 1951.

2. Edo News Notes. (Aviation Week, April 9, 1951, p. 34).

3. Underwater Flaps Aid Marlin. (Naval Aviation News, Navy Department, September 1950).

4. Martin Aircraft. (Aviation Week, January 29, 1951, p.44).

5. Libbey, L.B. The Effectiveness of Water Rudders on Flying Boats. Thesis at Stevens Institute of Technology, 1950.

6. Hugli, W.C., and Axt, W.C. Hydrodynamic Investigation of a Series of Hull Models Suitable for Small Flying Boats and Amphibians. Report No. 388, Experimental Towing Tank, Stevens Institute of Technology, 1949.

7. Locke, F.W.S., Jr. Some Yawing Tests of a 1/30-Scale Model of the Hull of the XPB2M-1 Flying Boat. NACA Report No. W-66, 1943.

8. Korvin-Kroukovsky, B.V. Hydrodynamic Design of Seaplanes. (Unedited Class Notes S.I.T. Course FD-215-216), Experimental Towing Tank, Stevens Institute of Technology, 1950.

9. Axt, W.C. Model Basin Tests of Several Devices for Reducing the Landing Run of a Flying Boat. Report No. 340, Experimental Towing Tank, Stevens Institute of Technology, 1948.

10. Smith, P.F., Gale, A.S., and Neelley, J.H. New Analytic Geometry. New York, Ginn and Company, Revised Edition.

11. Diehl, W.S. Engineering Aerodynamics. New York, The Ronald Press Company, 1940, Revised Edition.

TABLE Ia

TRIM AND YAW DATA UNDER STATIC CONDITIONS

C_Y	C_Δ	ψ in.-lb.	Ψ deg.	M_Ψ in.-lb.	τ deg.	α_p deg.	α_s deg.
			Bare Hull				
1.06	1.08	0.7	0	0	3.1	0	0
		0.7	1.1 s	0.5	3.1		
		1.5	2.1 s	0.5	3.0		
		1.5	3.3 s	1.5	3.0		
		0.7	4.4 s	2.0	3.1		
		0.7	2.85 s	1.3	3.1		
		0.7	1.7 s	1.0	3.1		
		0.7	0.55 s	0.3	3.1		
		0.7	1.1 p	0.5	3.1		
		1.5	3.4 p	2.0	3.0		
		0.7	2.2 p	1.0	3.1		
		-	1.7 p	1.0	-		
1.54	1.04	0	0	0	5.5		
		0	1.1 s	0.5	5.5		
		0	2.4 s	2.0	5.6		
		0	3.5 s	2.5	-		
		0	4.6 s	3.0	5.6		
		0	1.9 s	2.0	5.6		
		0	1.2 p	1.0	5.6		
		0	2.3 p	1.3	5.6		

TABLE Ib

C_V	C_Δ	M in.lb.	ψ deg.	M_ψ in.lb.	τ deg.	α_p deg.	α_s deg.
			Hull with Flaps On				
2.02	0.99	3.5	2.5 p	2.5	6.2	0	0
		2.0	1.2 p	1.0	6.1		
		0.5	0	0	6.0		
		1.5	1.2 s	1.0	6.1		
		1.5	2.5 s	2.5	6.2		
		2.5	3.9 s	4.5	6.3		
		-	5.0 s	5.0	6.7		
		2.0	0	0	5.8		
		-	1.2 s	0.8	-		
		2.0	2.5 s	2.5	6.1		
		-	1.2 p	1.0	-		
1.54	1.04	1.5	1.2 p	1.0	5.3		
		1.5	0	0	5.3		
		0.5	1.1 s	0.5	5.4		
		0.5	2.5 s	2.5	5.4		
1.06	1.08	1.5	2.2 s	1.0	3.0		
		-	1.1 s	2.5	-		
		1.5	0	0	3.0		
		1.5	1.1 p	0.5	3.0		

TABLE Ic

C_V	C_Δ	M in.lb.	ψ deg.	M_ψ in.lb.	γ deg.	α_p deg.	α_s deg.
		Hull with Flaps On; $\theta = 23^\circ$					
1.06	1.08	1.5	1.3 p	1.5	3.0	60	0
		1.5	2.5 p	2.5	3.0	60	
		1.5	0.1 p	0.5	3.0	30	0
		1.5	2.5 p	2.3	3.0		
		0.7	1.0 s	0	3.1		
		0.7	3.1 s	0.5	3.1		
		0.7	5.3 s	1.5	3.1		
		0.7	2.1 s	0.5	3.1		
1.54	1.04	- 1.5	2.0 s	0	5.7		
		- 1.5	4.1 s	0.5	5.7		
		0	0.5 p	2.5	5.6		
		0	1.6 p	3.0	5.6		
		0.5	2.8 p	4.0	5.5		
2.02	0.99	3.0	3.0 p	5.0	6.3		
		1.5	1.9 p	4.5	6.2		
		0.5	0.7 p	3.5	6.2		
		0.5	0.5 s	2.5	6.1		
		1.0	1.4 s	2.0	6.1		
		- 0.5	3.9 s	0.5	6.7		
		0	0	0	6.1	30	30
		1.5	3.0 s	0	6.2		
		2.5	3.0 p	0	6.2		

TABLE Id

C_V	C_Δ	M in.lb.	ψ deg.	M_ψ in.lb.	τ deg.	α_p deg.	α_s deg.
		Hull with Flaps On; $\theta = 23^\circ$					
1.54	1.04	0.7	0	0	5.4	30	30
		0.5	3.0 s		5.5		
		0.5	3.0 p		5.5		
1.06	1.08	1.5	3.0 p		3.0		
		1.5	0		3.0		
		1.5	3.0 s		3.0		
		1.5	0		3.0	60	60
		1.5	3.0 p		3.0		
		1.5	3.0 s		3.0		
1.54	1.04	0	3.0 p		5.6		
		0	0		5.6		
		- 1.5	3.0 s		5.7		
2.02	0.99	1.5	3.0 s		6.2		
		0	0		6.1		
		2.5	3.0 p		6.2		
		-10.0	3.0 s		7.8	90	90
		-10.5	0		7.4		
		- 9.5	3.0 p		7.8		
1.54	1.04	- 4.0	3.0 p		6.0		
		- 4.0	0		6.0		
		- 4.0	3.0 s		6.0		

TABLE Ie

C_V	C_Δ	M in.lb.	ψ deg.	M_ψ in.lb.	γ deg.	α_p deg.	α_s deg.
		Hull with Flaps On; $\theta = 23^\circ$					
1.06	1.08	0.7	0	0	3.1	90	90
		0.7	3.0 s		3.1		
		0.7	3.0 p		3.1		
2.02	0.99	0.5	1.5 p	7.5	6.3	90	0
		0	3.0 p	10.0	6.8		
		- 1.5	0.7 p	8.5	6.5		
		- 3.0	0.2 s	9.0	6.5		
		3.0	5.0 s	0	6.4		
		-	2.5 p	10.0	-		
			1.3 p	9.0	-		
1.54	1.04	0	1.2 p	6.0	5.6		
		- 2.5	2.3 p	6.7	5.8		
		- 1.5	0.1 p	5.5	5.7		
		- 2.5	2.0 s	4.5	5.8		
		- 2.5	4.1 s	4.5	5.8		
1.06	1.08	1.5	5.0 s	0	3.0		
		1.5	2.7 s	1.5	3.0		
		1.5	0.5 s	2.5	3.0		
		1.5	0.6 p	3.0	3.0		
		1.5	1.5 p	2.5	3.0		
		1.5	2.6 p	3.0	3.0		

TABLE If

C_V	C_Δ	M in.lb.	ψ deg.	M_ψ in.lb.	τ deg.	α_p deg.	α_s deg.
		Hull with Flaps On; $\theta = 23^\circ$					
2.02	0.99	0	1.0 p	5.0	6.3	60	0
		1.5	3.6 p	8.0	6.6		
		- 2.0	0.5 p	6.7	6.5		
		- 3.0	1.0 s	5.0	6.6		
		- 4.0	1.9 s	5.5	6.7		
		- 4.0	3.0 s	5.0	6.9		
1.54	1.04	- 1.5	3.0 p	5.0	5.7		
		- 1.5	1.9 p	4.5	5.7		
		- 2.5	0.8 p	4.0	5.8		
		- 3.5	0.4 s	3.0	5.9		
		- 3.5	1.4 s	3.0	5.9		
		- 3.5	3.5 s	2.5	5.9		
1.06	1.08	0.7	4.0 s	0	3.1		
		0.7	1.9 s	0.5	3.1		
		0.7	0.8 s	1.0	3.1		
		1.5	0.4 p	2.0	3.0		
		Hull with Flaps On; $\theta = 47^\circ$					
2.02	0.99	9.5	1.5 p	7.5	5.3	90	0
		8.0	2.7 p	8.5	5.7		
		9.5	4.0 p	10.0	5.9		
		8.0	0.5 p	7.5	5.2		

TABLE Ig

C_V	C_Δ	M in.lb.	ψ deg.	M_ψ in.lb.	τ deg.	α_p deg.	α_s deg.
		Hull with Flaps On; $\theta = 47^\circ$					
2.02	0.99	9.5	1.8 s	6.0	5.1	90	0
		9.5	4.0 s	4.5	5.5		
1.54	1.04	4.0	4.8 s	1.0	5.0		
		3.0	3.5 s	2.5	5.1		
		2.5	1.3 s	3.5	5.2		
		2.5	0.9 p	4.5	5.2		
		-	2.1 p	5.4	-		
		3.0	3.1 p	5.4	5.1		
1.06	1.08	2.8	2.7 p	3.5	2.8		
		2.8	1.5 p	2.5	2.8		
		2.8	0.5 p	2.5	2.8		
		2.2	1.8 s	1.0	2.9		
		-	0.6 s	2.0	-		
		1.5	3.9 s	0.5	3.0		
		2.8	0.5 p	2.5	2.8	60	0
		2.2	1.6 p	3.0	2.9		
		2.2	2.7 p	3.5	2.9		
		2.2	1.8 s	1.0	2.9		
		2.2	4.0 s	0	2.9		
1.54	1.04	4.0	3.8 s	1.0	5.0		
		4.0	1.5 s	2.5	5.0		

TABLE Ih

C_V	C_Δ	M in.lb.	ψ deg.	M_ψ in.lb.	τ deg.	α_p deg.	α_s deg.
		Hull with Flaps On; $\theta = 47^\circ$					
1.54	1.04	3.0	0.8 p	4.0	5.1	60	0
		4.0	1.9 p	4.5	5.0		
		4.0	3.0 p	5.0	5.0		
2.02	0.99	8.0	3.7 p	8.5	5.8		
		7.0	2.3 p	6.5	5.7		
		7.0	1.1 p	5.4	5.5		
		8.2	1.1 s	4.5	5.2		
		9.0	3.1 s	4.5	5.2		
		3.5	0.6 p	3.0	5.8	30	0
		4.5	1.9 p	4.5	5.8		
		5.5	2.9 p	4.5	5.9		
		3.0	1.6 s	2.0	5.9		
		5.5	4.1 s	0	6.0		
1.54	1.04	0	4.3 s	1.0	5.5		
		- 1.0	1.9 s	0.5	5.6		
		0	0.8 p	4.0	5.5		
		0.7	1.8 p	4.0	5.4		
		- 1.0	2.8 p	4.0	5.6		
1.06	1.08	1.5	2.4 p	2.0	3.0		
		1.5	1.1 p	0.5	3.0		
		1.5	0.2 p	1.0	3.0		

TABLE Ii

C_V	C_Δ	M in.lb.	ψ deg.	M_ψ in.lb.	τ deg.	α_p deg.	α_s deg.
		Hull with Flaps On; $\theta = 47^\circ$					
1.06	1.08	1.0	2.0 s	0	3.1	30	0
		1.0	4.1 s	0.5	3.1		
		1.0	0		3.1	30	30
		1.5	3.0 p		3.0		
		1.0	3.0 s		3.0		
1.54	1.04	0.7	3.0 s		5.4		
		1.5	0		5.3		
		2.3	3.0 p		5.2		
2.02	0.99	8.0	3.0 p		5.8		
		5.0	0		5.5		
		6.0	3.0 s		5.8		
		10.5	0		4.8		
		11.5	3.0 s		5.0		
		13.5	3.0 p		5.0		
1.54	1.04	4.0	0		5.0		
		5.5	3.0 p		4.8		
		4.7	3.0 s		4.9		
1.06	1.08	3.5	3.0 s		2.7		
		4.7	0		2.5		
		3.5	3.0 p		2.7		
		2.2	0		2.9	90	90

TABLE Ij

C_V	C_Δ	M in.lb.	ψ deg.	M_ψ in.lb.	τ deg.	α_p deg.	α_s deg.
		Hull with Flaps On; $\theta = 47^\circ$					
1.06	1.08	2.8	3.0 p		2.8	90	90
		2.8	3.0 s		2.8		
1.54	1.04	4.0	3.0 s		5.0		
		3.0	0		5.1		
		4.0	3.0 p		5.0		
2.02	0.99	13.0	3.0 p		5.1		
		12.5	0		4.5		
		11.5	3.0 s		5.1		
		Hull with Flaps On; $\theta = 60^\circ$					
2.02	0.99	2.5	0.6 p	3.0	5.9	30	0
		4.5	1.8 p	4.0	5.9		
		6.0	2.9 p	4.5	6.0		
		5.0	1.8 s	1.0	5.8		
		6.5	4.0 s	0	5.9		
1.54	1.04	2.3	4.1 s	0.5	5.2		
		2.3	1.9 s	0	5.2		
		1.5	0.3 p	1.25	5.3		
		0.7	1.5 p	2.5	5.4		
		0	2.6 p	3.0	5.5		
1.06	1.08	1.5	2.5 p	2.5	3.0		
		1.5	1.3 p	1.5	3.0		

TABLE Ik

C_V	C_Δ	M in.lb.	ψ deg.	M_ψ in.lb.	τ deg.	α_p deg.	α_s deg.
		Hull with Flaps On; $\theta = 60^\circ$					
1.06	1.08	1.5	0.2 p	1.0	3.0	30	0
		1.5	2.0 s	0	3.0		
		1.5	4.1 s	0.5	3.0		
		2.2	0.5 p	2.5	2.9	60	0
		2.0	1.5 p	2.5	2.9		
		2.2	2.6 p	3.0	2.9		
		2.2	0.8 s	1.0	2.9		
		2.8	3.0 s	0	2.8		
1.54	1.04	4.0	2.8 s	1.0	5.0		
		3.0	0.4 s	3.0	5.1		
		2.3	0.8 p	4.0	5.2		
		2.3	1.9 p	4.5	5.2		
		2.3	3.0 p	5.0	5.2		
2.02	0.99	11.0	3.9 p	9.5	5.6		
		8.5	2.5 p	7.5	5.6		
		8.5	1.2 p	6.0	5.3		
		8.0	0	5.0	5.1		
		11.0	2.1 s	4.5	5.0		
		12.5	4.0 s	2.5	5.0		
		9.5	1.5 p	7.5	5.1	90	0
		10.0	2.9 p	9.5	5.5		

TABLE I1

C_V	C_Δ	M in.lb.	ψ deg.	M_ψ in.lb.	τ deg.	α_p deg.	α_s deg.
		Hull with Flaps On; $\theta = 60^\circ$					
2.02	0.99	9.0	4.2 p	11.0	5.9	90	0
		9.0	0.3 p	6.6	5.1		
		9.5	0.8 s	6.0	5.0		
		9.5	4.4 s	3.5	5.5		
		10.0	2.5 s	5.0	5.2		
1.54	1.04	2.3	3.0 s	2.5	5.2		
		1.5	0.1 s	4.5	5.3		
		1.5	0.9 p	4.5	5.3		
		1.5	2.0 p	5.0	5.3		
		1.5	3.1 p	5.5	5.3		
1.06	1.08	1.5	2.5 p	2.5	3.0		
		1.5	1.5 p	2.5	3.0		
		1.5	0.5 p	2.5	3.0		
		1.5	0.8 s	1.0	3.0		
		1.5	3.0 s	0	3.0		
		4.0	0		2.6	90	90
		4.7	3.0 s		2.5		
		4.7	3.0 p		2.5		
1.54	1.04	10.2	3.0 p		4.2		
		9.5	0		4.3		
		10.2	3.0 s		4.2		

TABLE Im

C_V	C_Δ	M in.lb.	ψ deg.	M_ψ in.lb.	τ deg.	α_p deg.	α_s deg.
		Hull with Flaps On; $\theta = 60^\circ$					
2.02	0.99	17.5	3.0 s	0	4.1	90	90
		17.5	0		3.8		
		19.5	3.0 p		4.1		
		16.5	0		4.0	60	60
		16.5	3.0 s		4.2		
		18.0	3.0 p		4.2		
1.54	1.04	9.5	3.0 p		4.3		
		8.8	0		4.4		
		9.5	3.0 s		4.3		
1.06	1.08	4.7	3.0 s		2.5		
		3.5	0		2.7		
		4.7	3.0 p		2.5		
		2.2	0		2.9	30	30
		1.5	3.0 s		3.0		
		2.2	3.0 p		2.9		
1.54	1.04	3.0	3.0 p		5.1		
		2.3	0		5.2		
		3.0	3.0 s		5.1		
2.02	0.99	9.5	3.0 s		5.4		
		7.5	0		5.2		
		10.5	3.0 p		5.4		

TABLE In

C_V	C_Δ	M in.lb.	ψ deg.	M_ψ in.lb.	τ deg.	α_p deg.	α_s deg.
Hull with Flaps On; $\theta = 34^\circ$							
1.06	1.08		0.1 p	0.5		30	0
			2.4 p	2.0			
			1.2 p	1.0			
			0.9 s	0.5			
1.54	1.04		0.5 s	2.5			
			0.7 p	3.5			
			1.75 p	3.75			
2.02	0.99		0.5 p	2.5			
			0.7 s	1.25			
			0.5 p	5.0			
			0.1 p	5.5			
			1.4 p	7.0			
			0.1 p	5.5			
			1.1 s	4.5			
			0.9 p	4.5		60	0
			1.1 p	10.5			
			0.1 p	10.5			
1.54	1.04		0.9 s	5.5			
			0.5 p	7.5			
			1.5 p	7.5			
1.06	1.08		0.5 p	2.5			

TABLE Io

C_V	C_Δ	M in.lb.	ψ deg.	M_ψ in.lb.	τ deg.	α_p deg.	α_s deg.
Hull with Flaps On; $\theta = 60^\circ$							
1.06	1.08		0.5 s	2.5		60	0
			1.6 p	3.0			
			0.6 p	3.0		90	0
			0.5 s	2.5			
			1.8 p	4.0			
1.54	1.04		2.8 p	9.0			
			1.7 p	8.5			
			0.7 p	8.5			
			0.4	8.0			
2.02	0.99		0.2 p	11.0			
			1.6 p	13.0			
			0.6 p	12.0			

TABLE IIa

APPLIED MOMENT VS. TRIM DATA

C_V	C_Δ	M in.lb.	ψ deg.	τ deg.
		Bare Hull		
1.54	1.04	0	3 s	5.6
		7.63	3 s	4.6
		15.3	3 s	3.5
		-22	3 s	8.1
		-11	3 s	6.8
		-11	0	6.8
		-22	0	8.1
		15.3	0	3.5
		15.3	5 p	3.5
		-22	5 p	8.1
1.06	1.08	-22	5 p	6.0
		-11	5 p	4.8
		7.6	5 p	2.0
		15.3	5 p	0.9
		15.3	0	0.9
		-22	0	6.0
		0	0	3.2
		0	5 s	3.1
		-22	5 s	6.0
		15.3	5 s	0.9

TABLE IIb

C_V	C_Δ	M in.lb.	ψ deg.	τ deg.
		Bare Hull		
2.02	0.99	15.3	5 s	4.6
		7.6	5 s	5.8
		-11	5 s	8.1
		-22	5 s	10.1
		0	0	6.1
		-11	0	7.3
		7.6	0	5.3
		15.3	0	4.3
		-22	0	9.1
		0	5 s	6.6
		0	5 p	7.0
		-11	5 p	8.8
		7.6	5 p	6.0
		15.3	5 p	5.0
		-22	5 p	10.2

TABLE III

RESISTANCE DATA

$\Psi = 0^{\circ}; \alpha_p = \alpha_s$

	$C_V = 1.06$		$C_V = 2.02$	
α	τ	R	τ	R
deg.	deg.	lb.	deg.	lb.
		$\theta = 47^{\circ}$		
90	2.9	0.465	4.5	1.47
60	2.5	0.415	5.0	1.29
30	3.1	0.38	5.5	1.13
		$\theta = 60^{\circ}$		
30	2.9	0.37	5.2	1.15
60	2.7	0.46	4.0	1.46
90	2.6	0.52	3.8	1.71
		Bare Hull		
	3.0	3.3	5.8	1.08

TABLE IV

SOLUTION OF ANALYTICAL FORMULA FOR PITCHING MOMENT COEFFICIENTS

α	$\theta = 21^\circ$	$\theta = 47^\circ$	$\theta = 59^\circ$
	C_M at $\beta = 20^\circ$		
0	0	0	0
15	-0.0874	-0.1665	-0.2019
30	-0.1382	-0.2789	-0.3483
45	-0.1393	-0.3052	-0.3984
60	-0.0895	-0.2400	-0.3390
75	-0.0028	-0.0996	-0.1870
90	+0.0976	+0.0772	+0.0180
	C_M at $\beta = 40^\circ$		
0	0	0	0
30	-0.0795	-0.184	-0.250
60	+0.0275	-0.070	-0.160
90	+0.2120	+0.230	+0.147

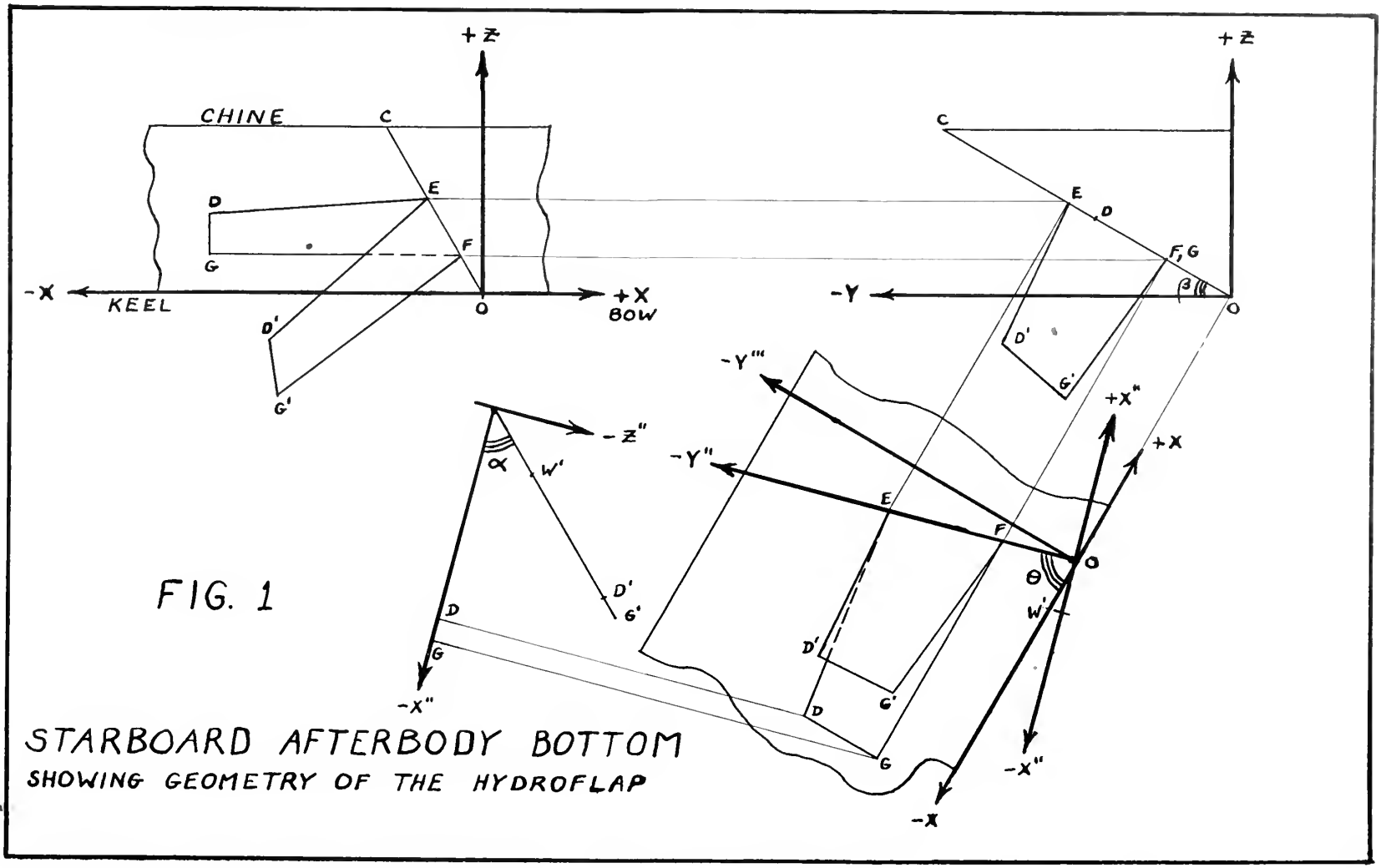

FIG. 1

STARBOARD AFTERBODY BOTTOM

SHOWING GEOMETRY OF THE HYDROFLAP

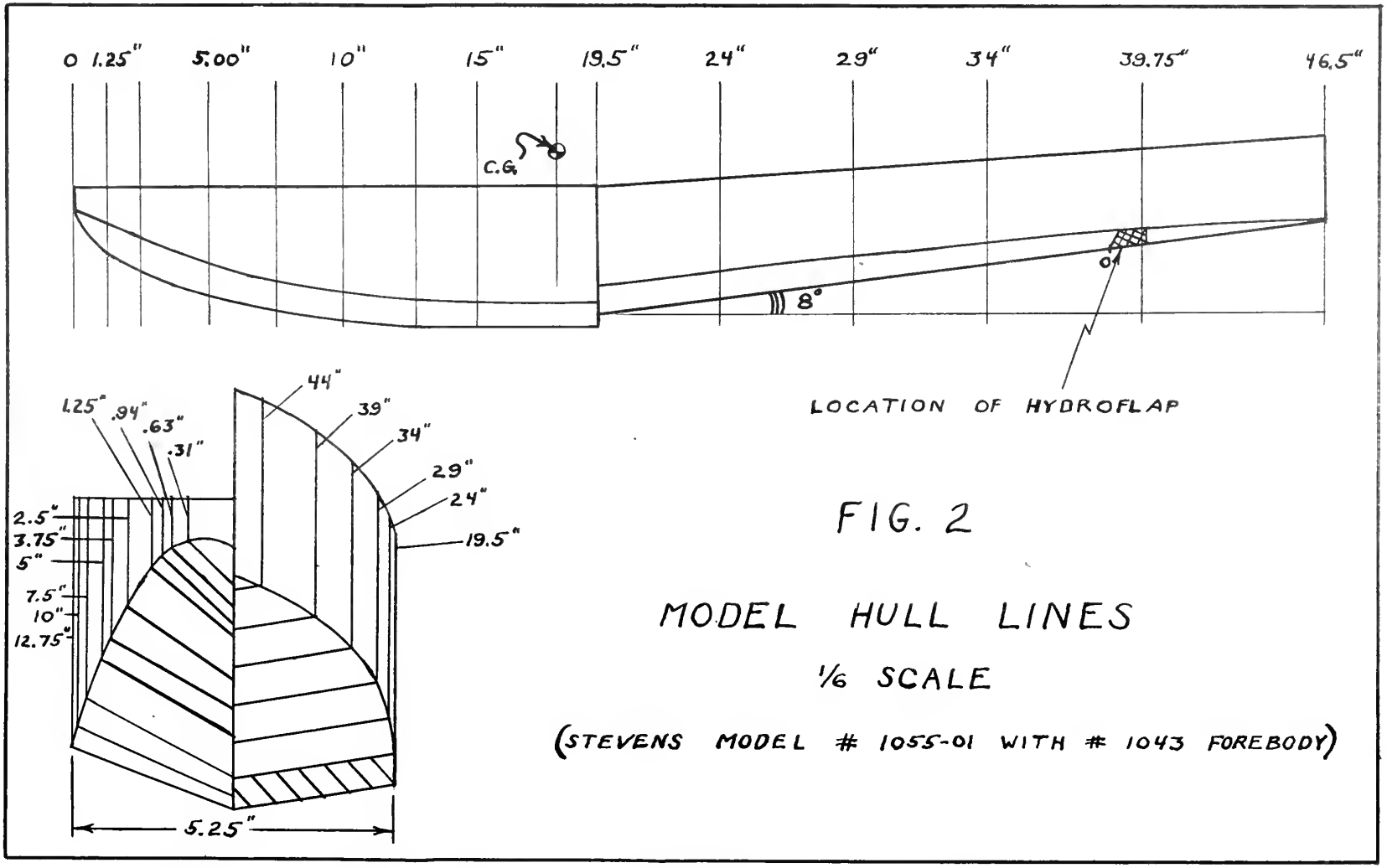

FIG. 2

MODEL HULL LINES

1/6 SCALE

(STEVENS MODEL # 1055-01 WITH # 1043 FOREBODY)

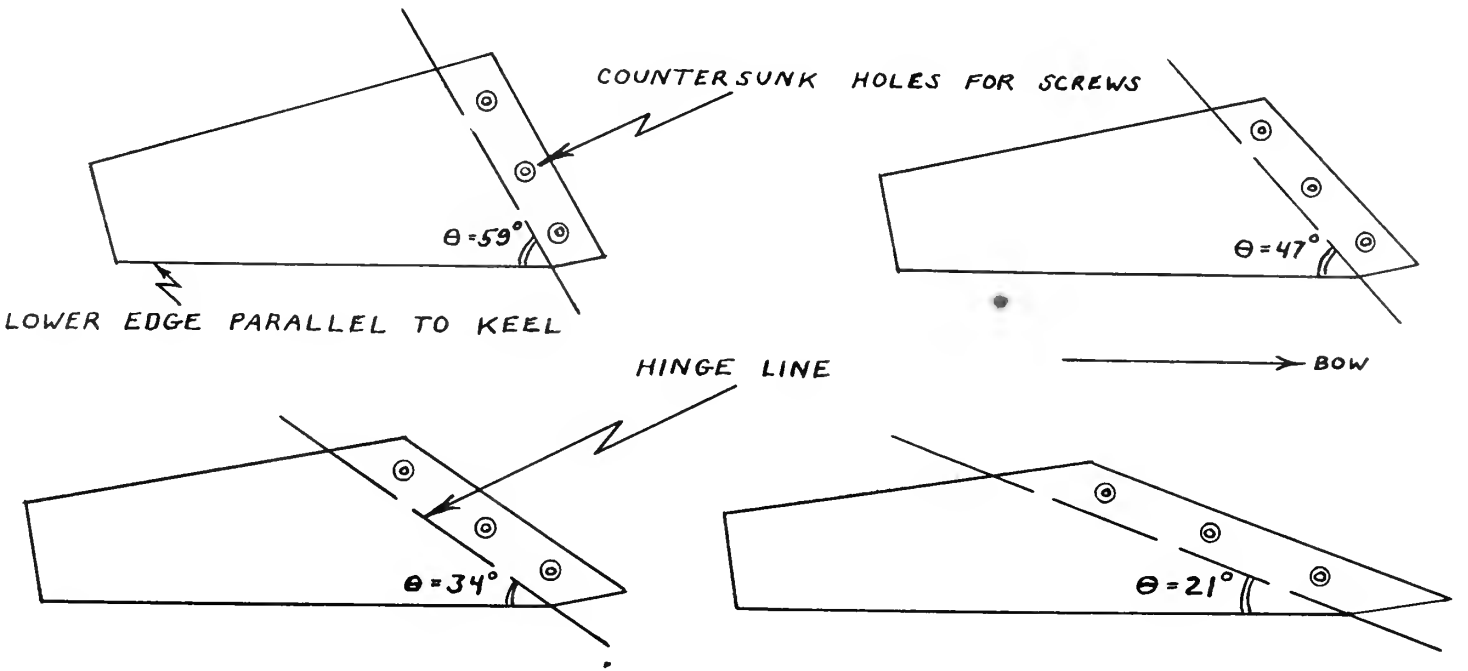

FIG. 3

HYDROFLAPS USED IN TANK TESTS

FULL SCALE

HYDROFLAP ON AFTERBODY BOTTOM

Side view

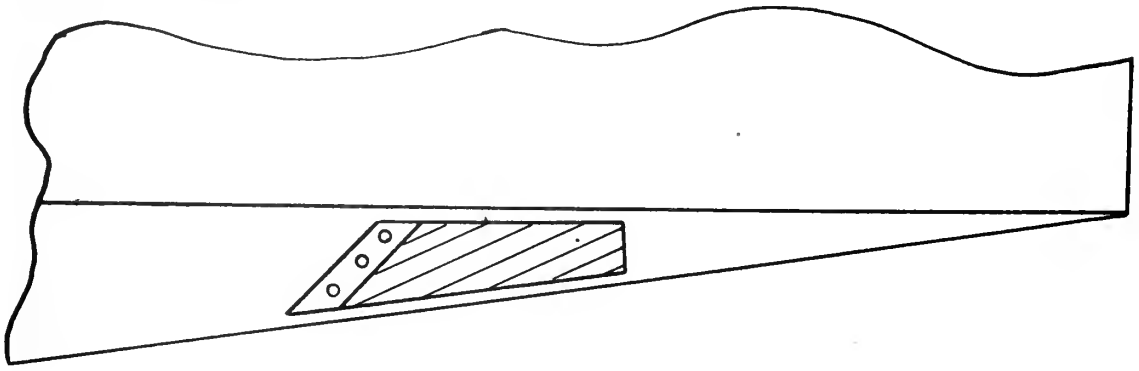

Bottom view

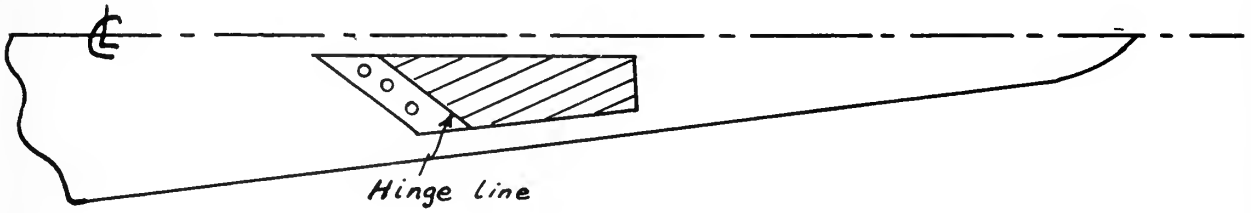

Geometry of hydroflap on afterbody bottom indicating angles α, β, and Θ.

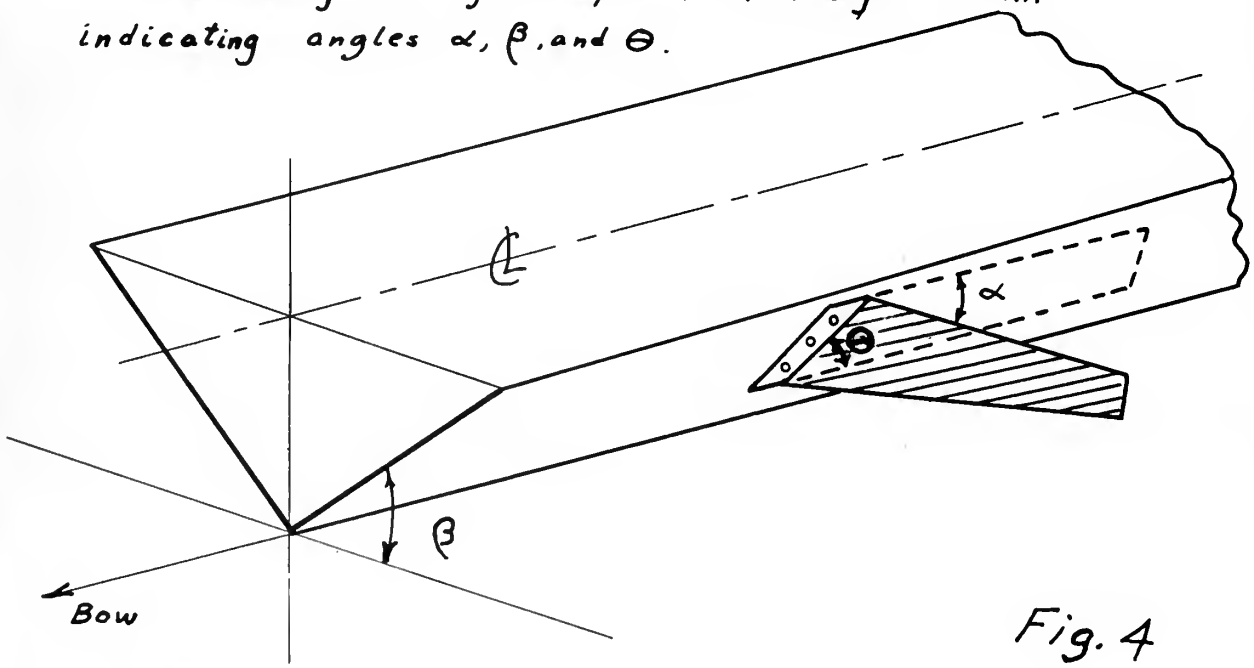

Fig. 4

SCHEMATIC SKETCH OF YAWING AND TRIM APPARATUS

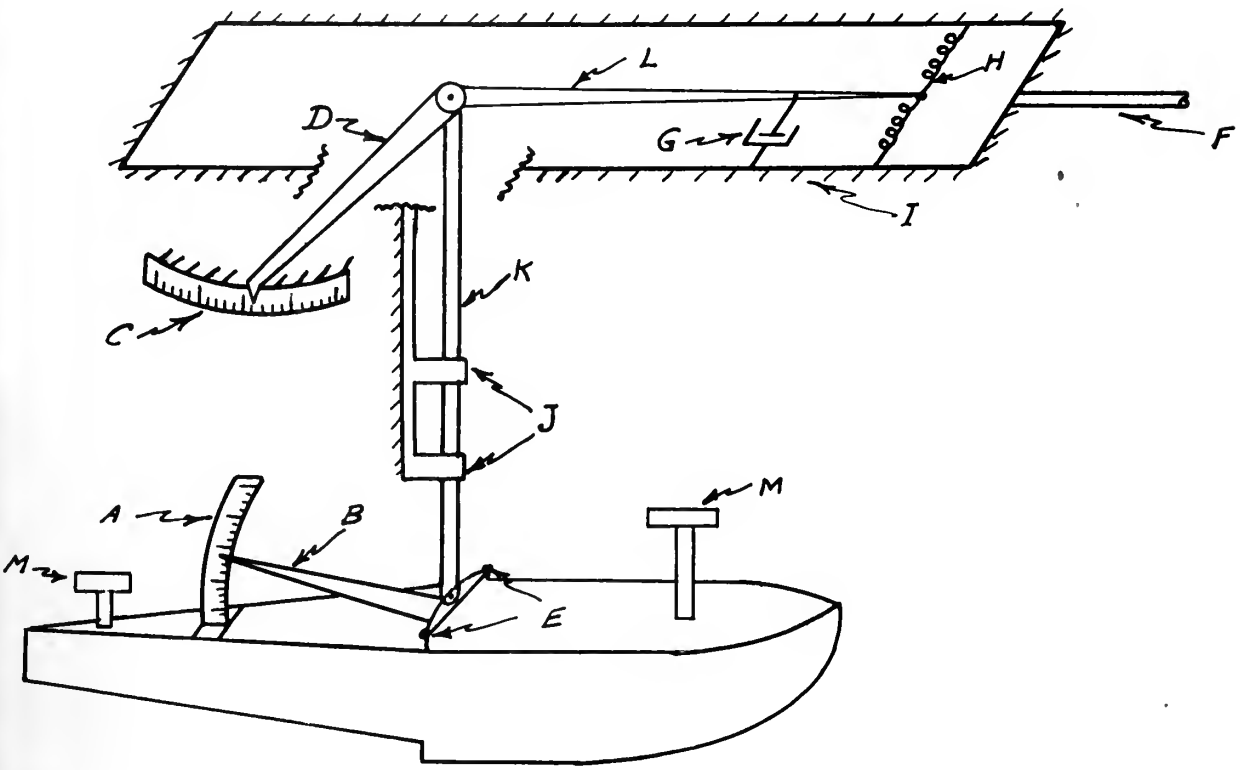

A	Trim scale
B	Trim pointer
C	Yaw scale
D	Yaw pointer
E	C.G. axis and pivot points (free to pitch)
F	Towing arm
G	Yaw damping
H	Calibrated Yaw moment spring
I	Main towing gate
J	Bearings to support shaft (K)
K	Model support shaft (free to rotate about vertical axis)
L	Torque arm attached to Yaw pointer (D) pivoted on shaft (K)
M	Weight mast

Fig. 5

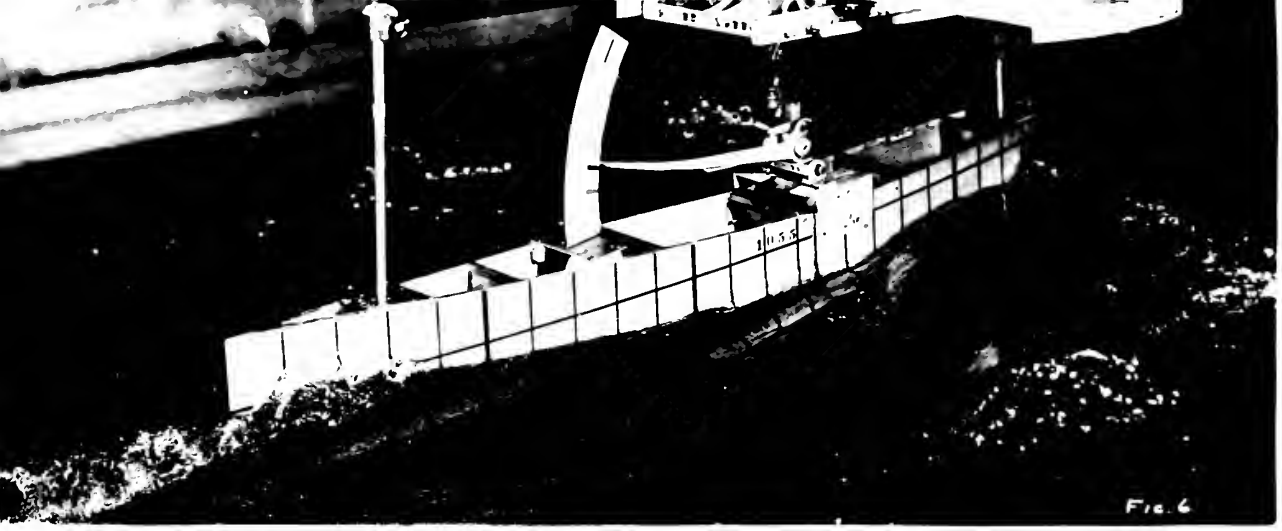

Fig. 6

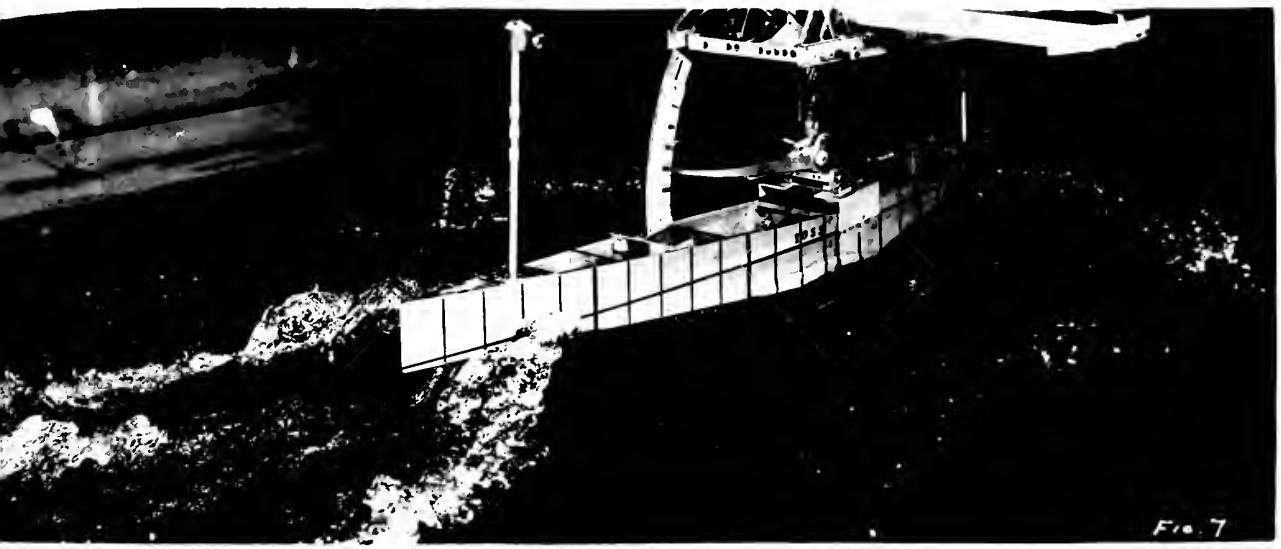

Fig. 7

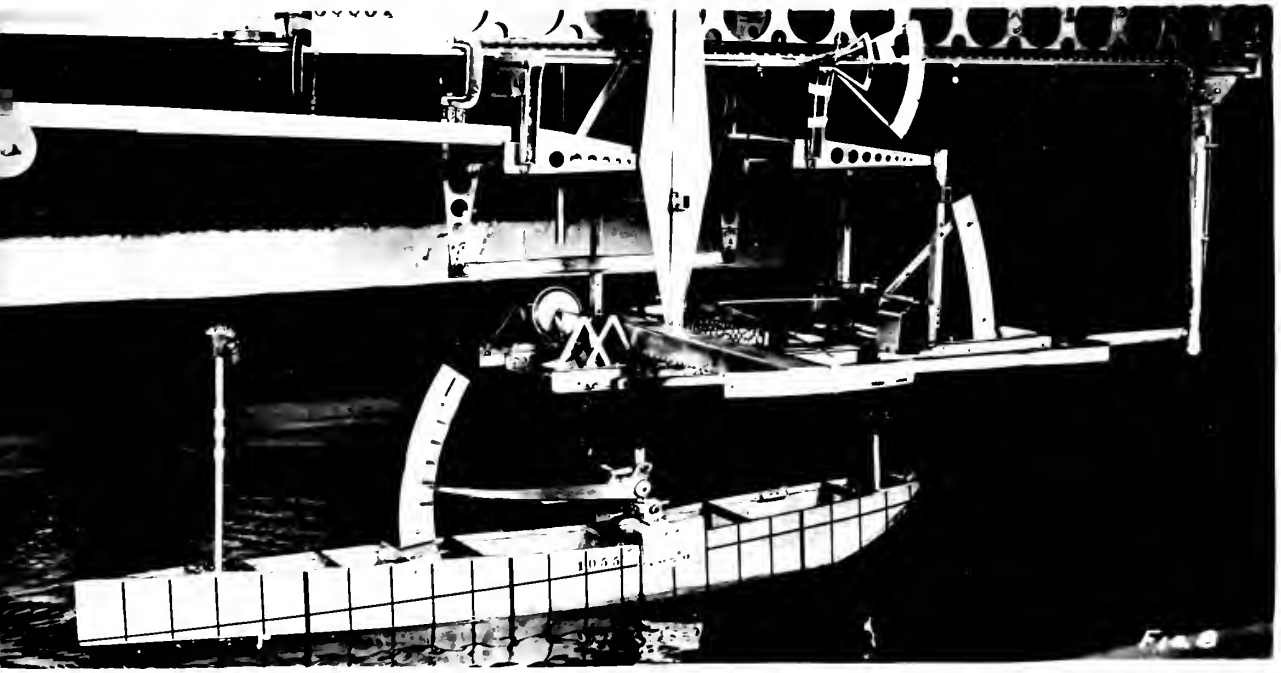

Fig. 8

SCHEMATIC SKETCH OF RESISTANCE APPARATUS

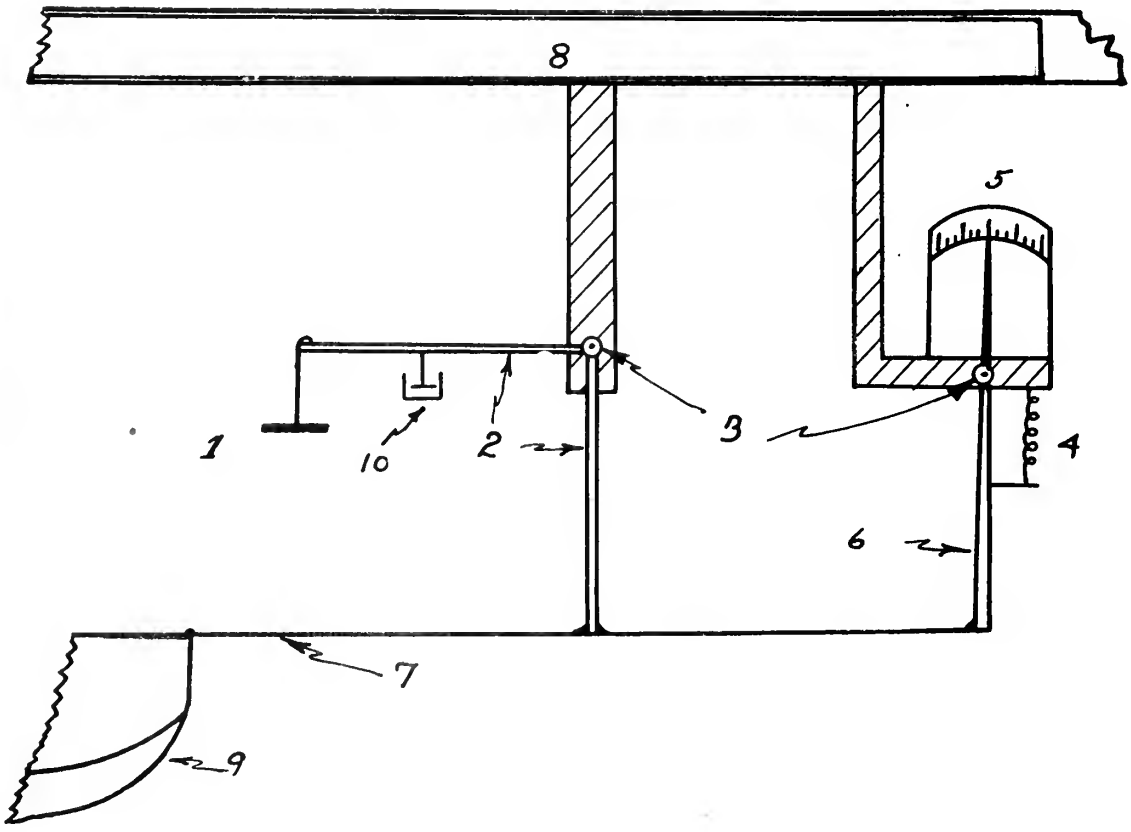

1	Weight pan
2	Bell crank lever
3	Pivot points
4	Calibrated spring
5	Spring scale
6	Pointer
7	Towing arm
8	Carriage
9	Model
10	Dashpot

Fig. 9

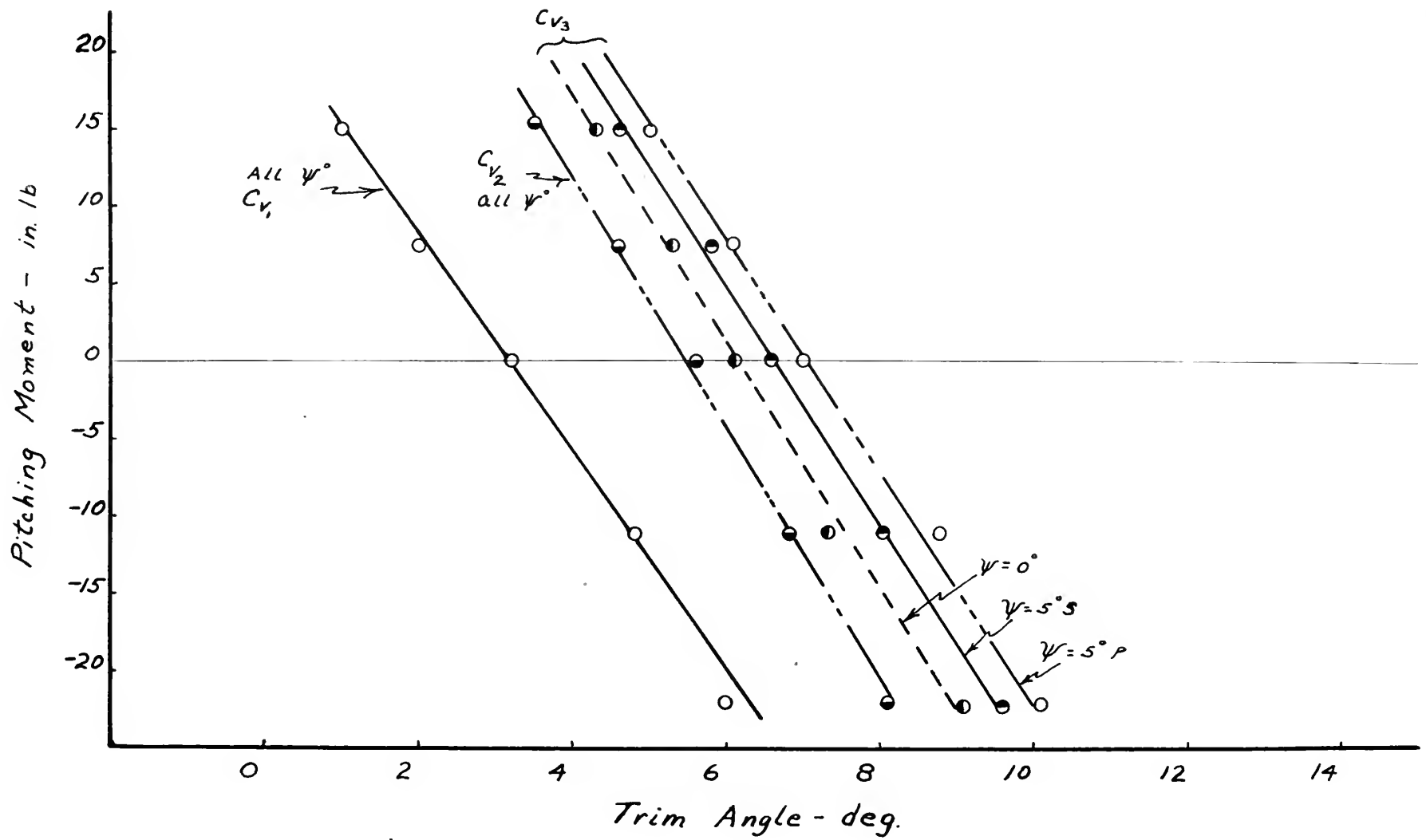
Applied Pitching Moment Vs. Trim Angle
C_{V_1}, C_{V_2}, C_{V_3} and $\Psi°$
C_{V_3}
All $\Psi°$
C_{V_1}
C_{V_2}
all $\Psi°$
$\Psi = 0°$
$\Psi = 5°S$
$\Psi = 5°P$
Pitching Moment - in. lb
20
15
10
5
0
-5
-10
-15
-20
0
2
4
6
8
10
12
14
Trim Angle - deg.

Fig. 10

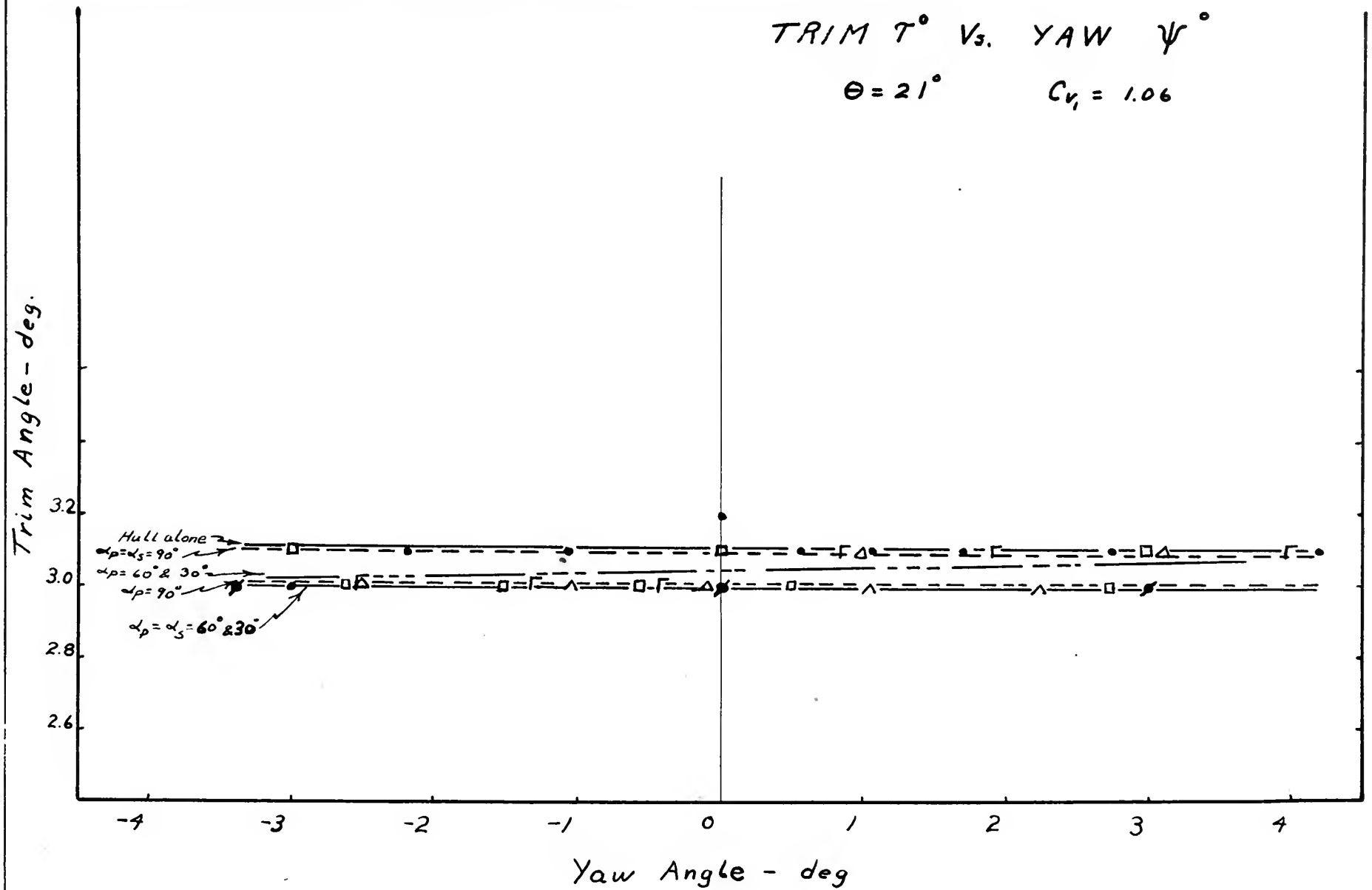
TRIM T° Vs. YAW ψ°
Θ = 21°
C_{V_1} = 1.06
Trim Angle - deg.
3.2
3.0
2.8
2.6
Hull alone
$\alpha_p = \alpha_s = 90°$
$\alpha_p = 60° \& 30°$
$\alpha_p = 90°$
$\alpha_p = \alpha_s = 60° \& 30°$
-4
-3
-2
-1
0
1
2
3
4
Yaw Angle - deg

Fig. 11

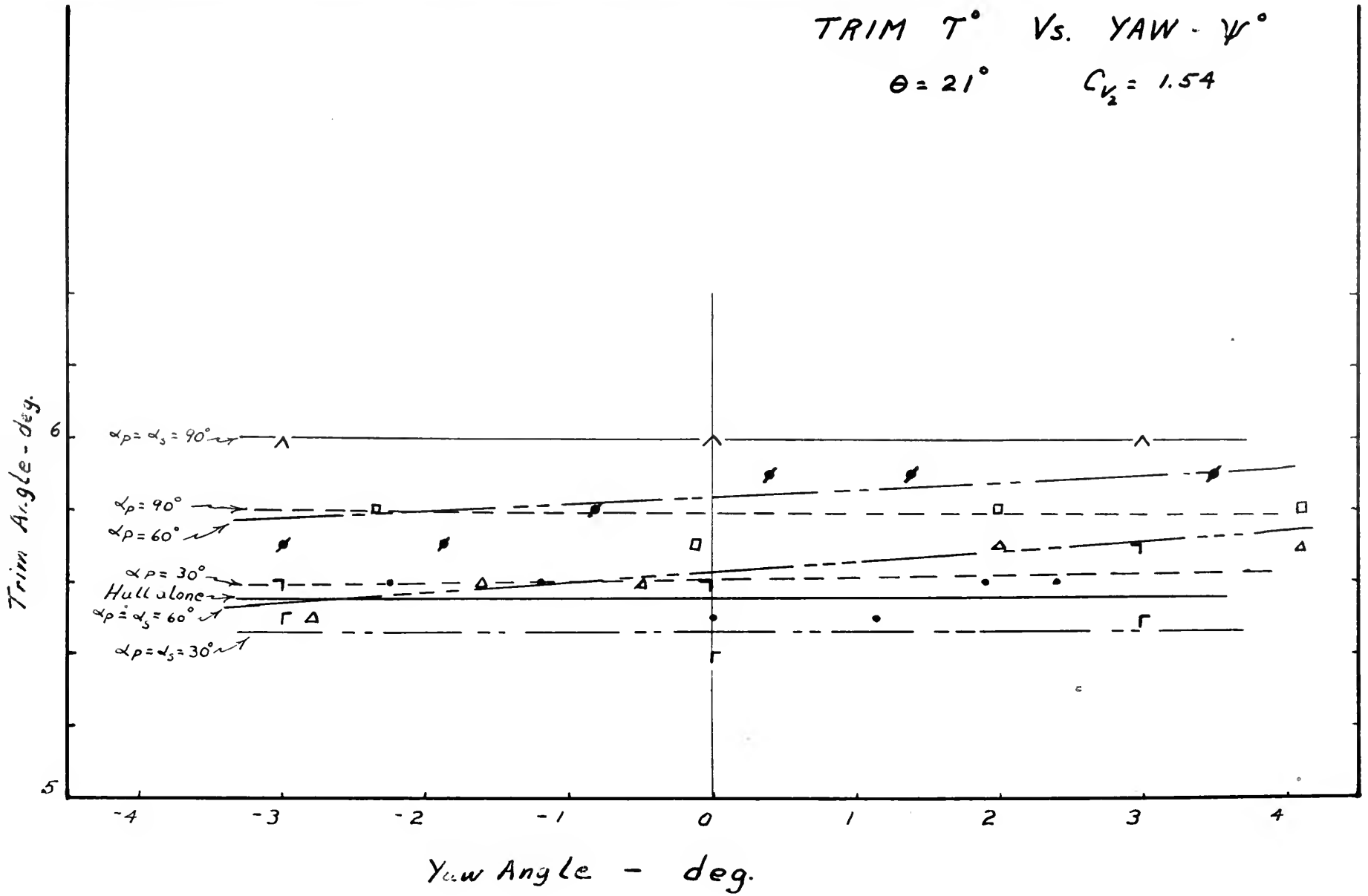
TRIM T° Vs. YAW - ψ°
θ = 21°
C_{V_2} = 1.54
Trim Angle - deg.
6
5
$\alpha_p = \alpha_s = 90°$
$\alpha_p = 90°$
$\alpha_p = 60°$
$\alpha_p = 30°$
Hull alone
$\alpha_p = \alpha_s = 60°$
$\alpha_p = \alpha_s = 30°$
-4
-3
-2
-1
0
1
2
3
4
Yaw Angle - deg.

Fig. 12

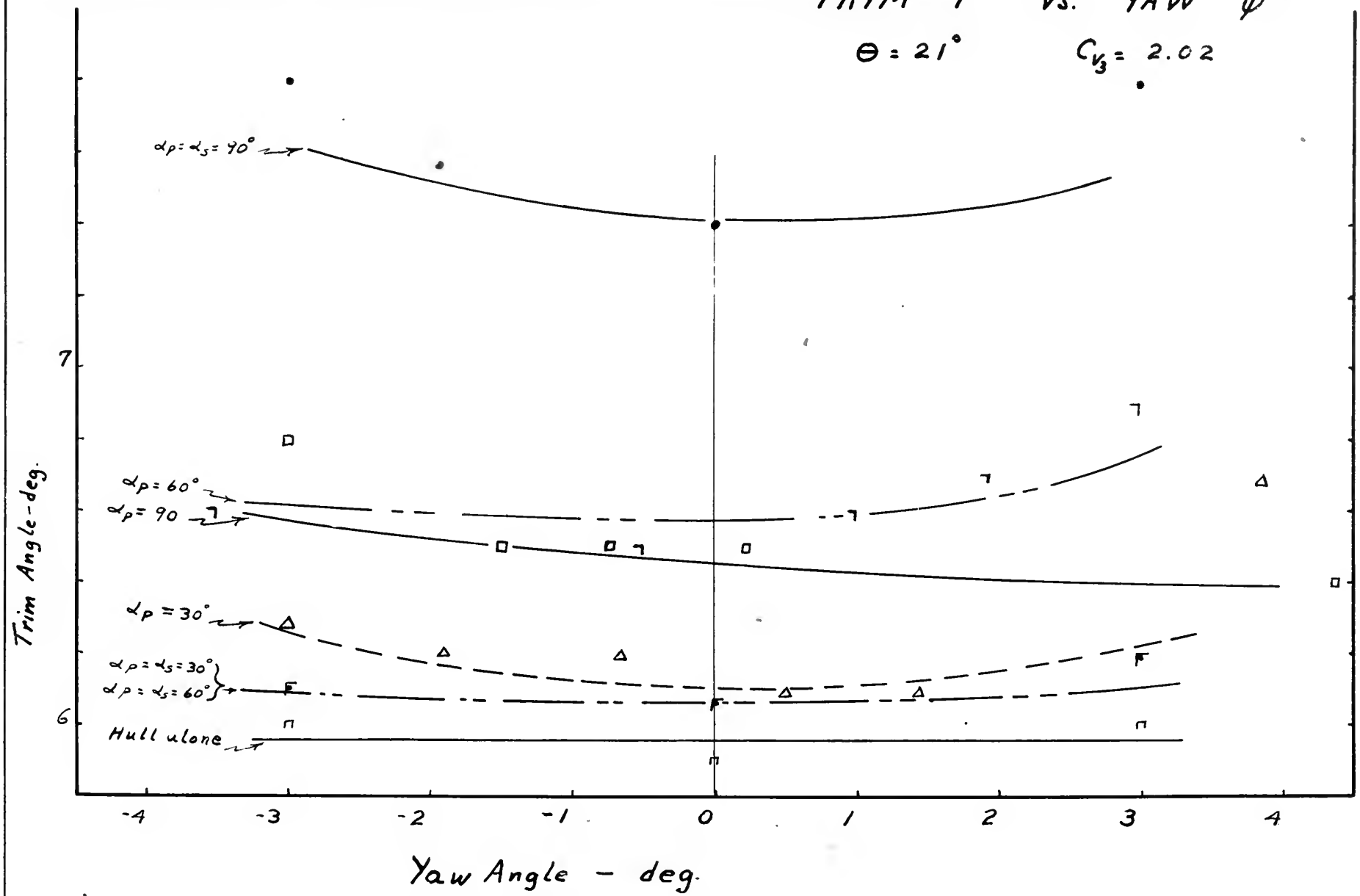
TRIM T° Vs. YAW ψ°
Θ = 21°
C_{V_3} = 2.02
$\alpha_p = \alpha_s = 90°$
$\alpha_p = 60°$
$\alpha_p = 90$
$\alpha_p = 30°$
$\alpha_p = \alpha_s = 30°$
$\alpha_p = \alpha_s = 60°$
Hull alone
7
6
Trim Angle - deg.
-4
-3
-2
-1
0
1
2
3
4
Yaw Angle - deg.

Fig. 13

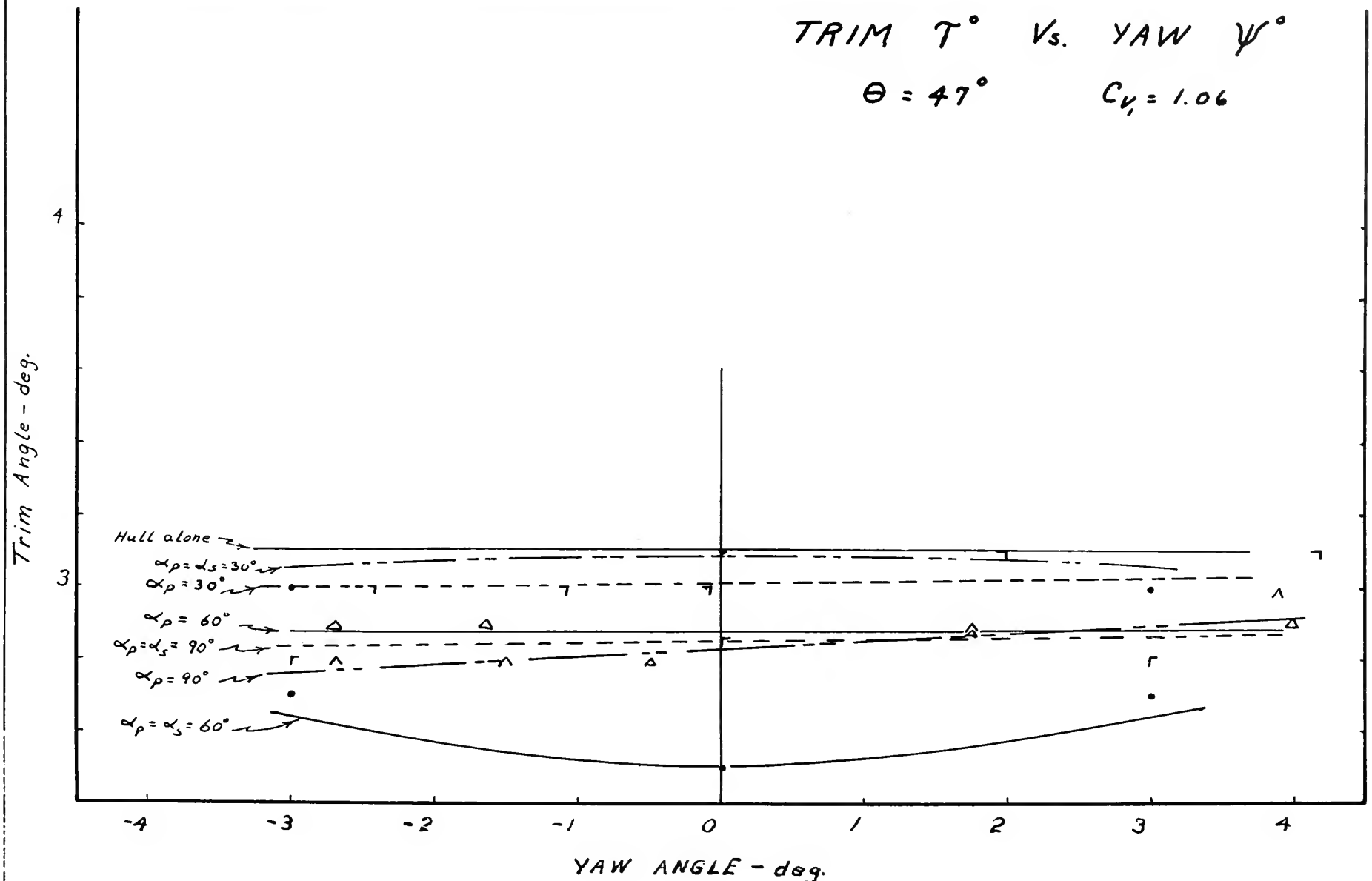
TRIM T° Vs. YAW Ψ°
Θ = 47°
C_{V_1} = 1.06
Trim Angle - deg.
4
3
Hull alone
$\alpha_p = \alpha_s = 30°$
$\alpha_p = 30°$
$\alpha_p = 60°$
$\alpha_p = \alpha_s = 90°$
$\alpha_p = 90°$
$\alpha_p = \alpha_s = 60°$
-4
-3
-2
-1
0
1
2
3
4
YAW ANGLE - deg.

Fig. 14

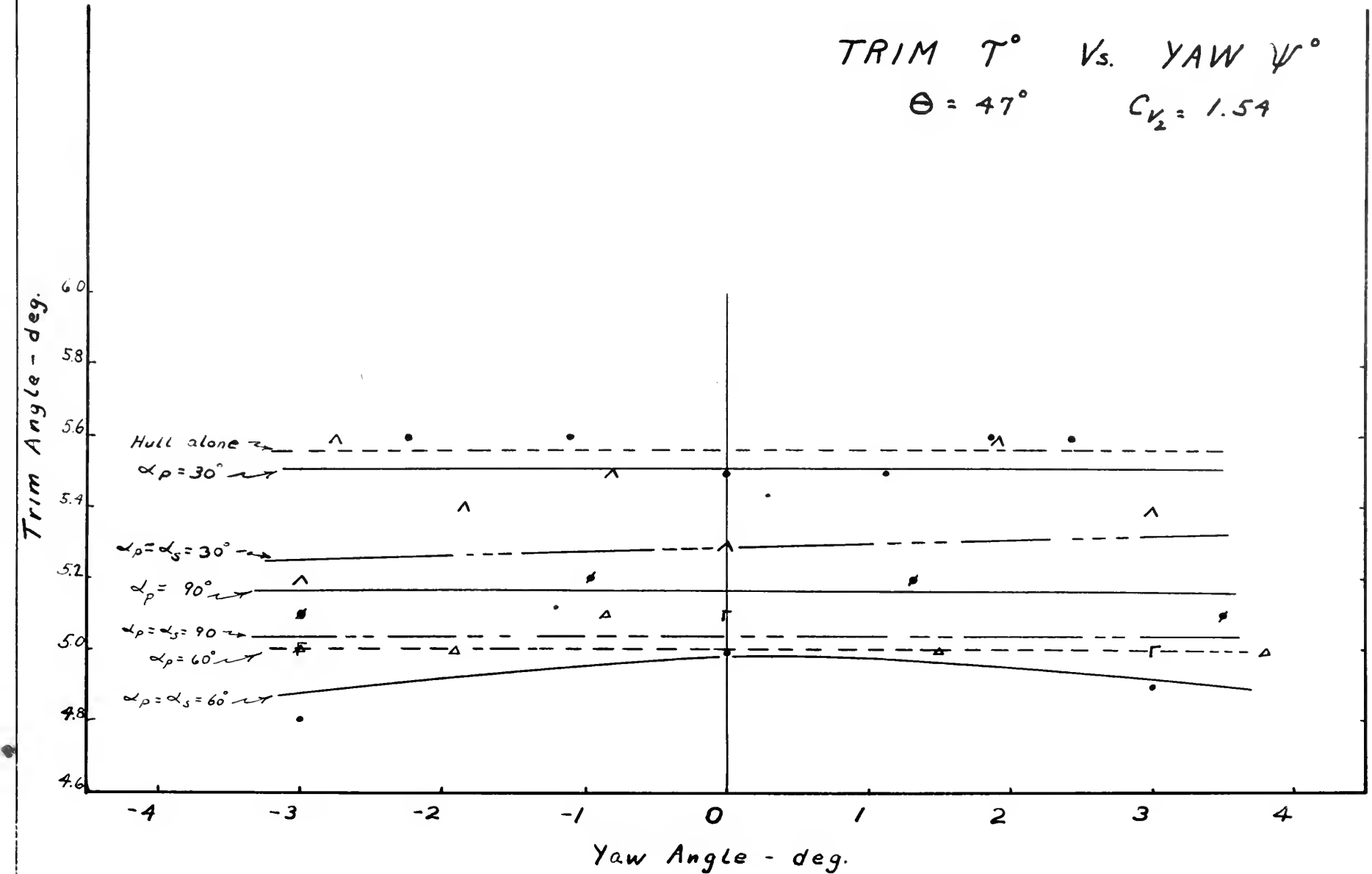
TRIM T° Vs. YAW ψ°
Θ = 47°
C_{V_2} = 1.54
Trim Angle - deg.
6.0
5.8
5.6
5.4
5.2
5.0
4.8
4.6
Hull alone
$\alpha_p = 30°$
$\alpha_p = \alpha_s = 30°$
$\alpha_p = 90°$
$\alpha_p = \alpha_s = 90$
$\alpha_p = 60°$
$\alpha_p = \alpha_s = 60°$
-4
-3
-2
-1
0
1
2
3
4
Yaw Angle - deg.

Fig. 15

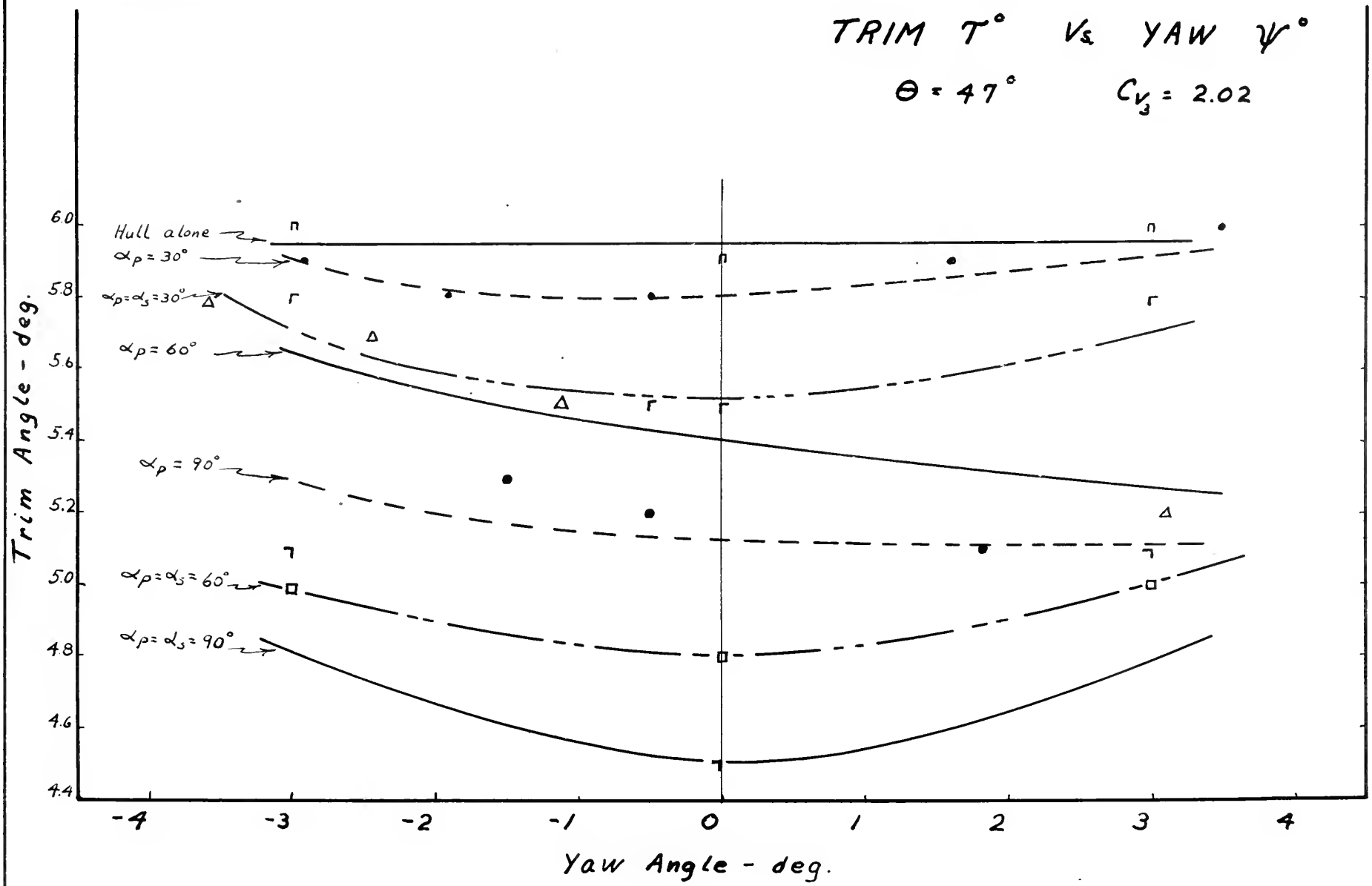
TRIM T° Vs YAW ψ°
θ = 47°
C_{V_3} = 2.02
Hull alone
α_p = 30°
$\alpha_p = \alpha_s$ = 30°
α_p = 60°
α_p = 90°
$\alpha_p = \alpha_s$ = 60°
$\alpha_p = \alpha_s$ = 90°
Trim Angle - deg.
6.0
5.8
5.6
5.4
5.2
5.0
4.8
4.6
4.4
-4
-3
-2
-1
0
1
2
3
4
Yaw Angle - deg.

Fig. 16

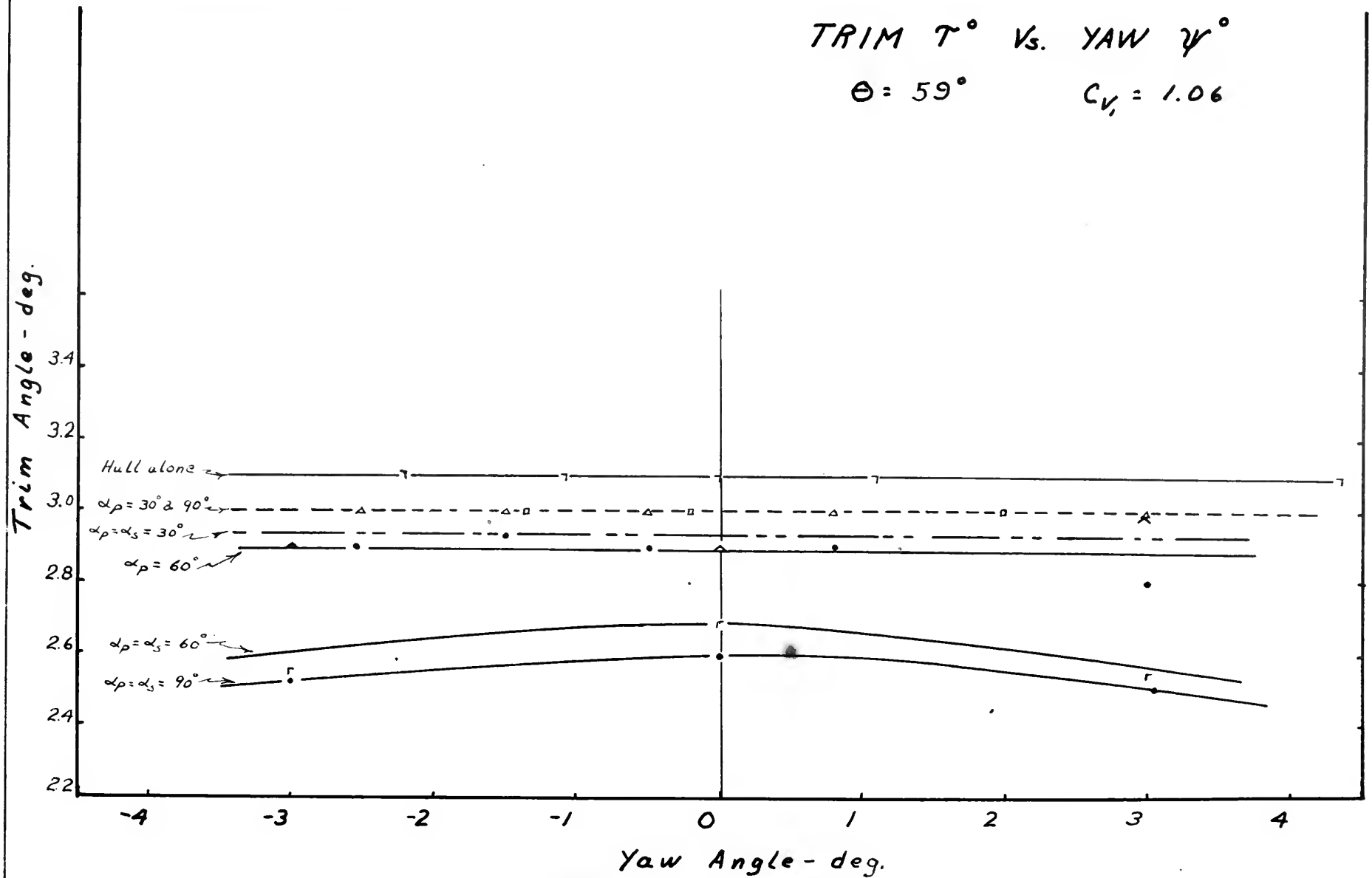
TRIM T° Vs. YAW ψ°
θ = 59°
C_{V_1} = 1.06
Trim Angle - deg.
3.4
3.2
3.0
2.8
2.6
2.4
2.2
Hull alone
α_p = 30° & 90°
$\alpha_p = \alpha_s$ = 30°
α_p = 60°
$\alpha_p = \alpha_s$ = 60°
$\alpha_p = \alpha_s$ = 90°
-4
-3
-2
-1
0
1
2
3
4
Yaw Angle - deg.

Fig. 17

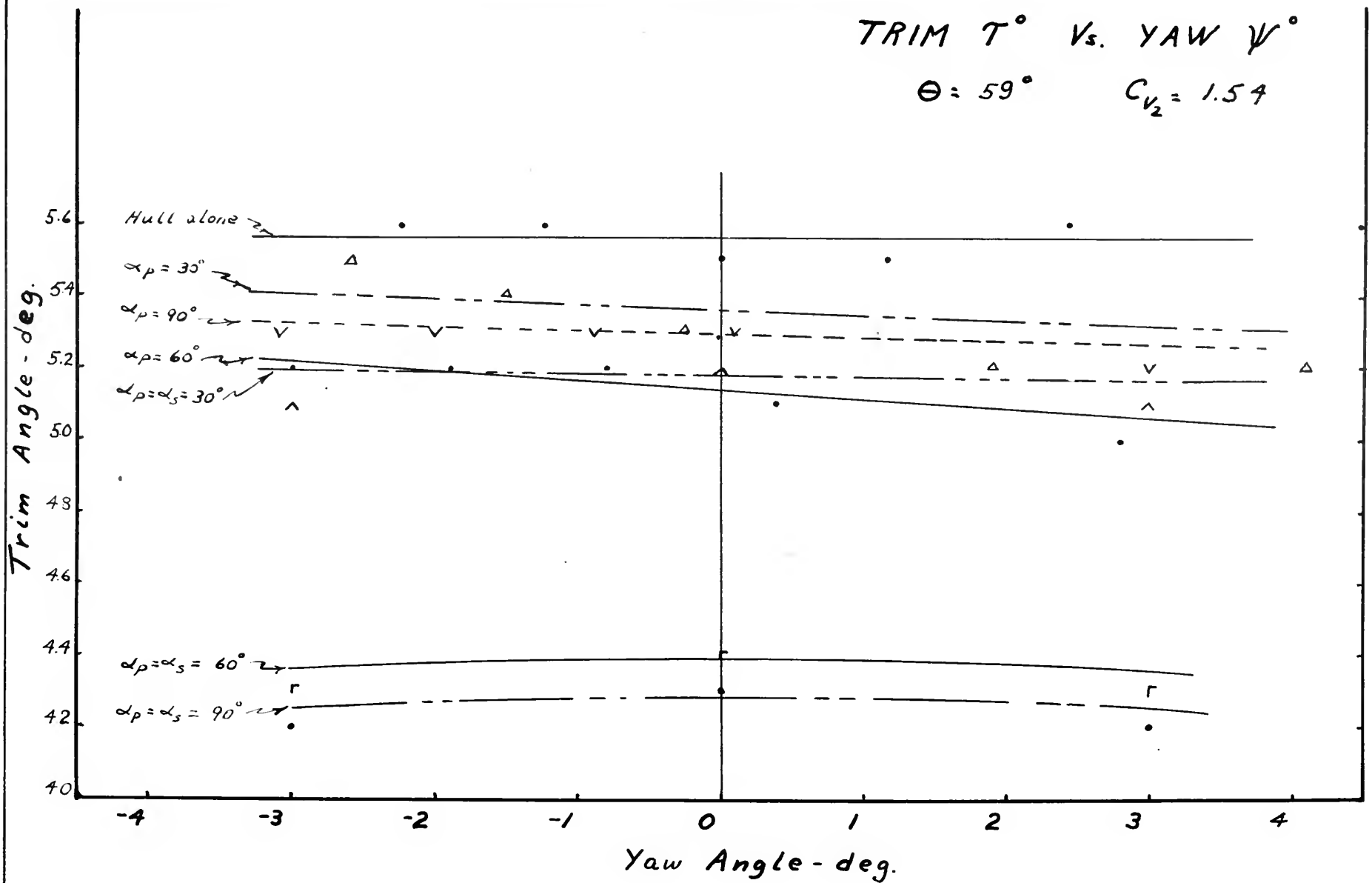
TRIM T° Vs. YAW Ψ°
Θ = 59°
C_{V_2} = 1.54
Hull alone
α_p = 30°
α_p = 90°
α_p = 60°
$\alpha_p = \alpha_s$ = 30°
$\alpha_p = \alpha_s$ = 60°
$\alpha_p = \alpha_s$ = 90°
Trim Angle - deg.
5.6
5.4
5.2
5.0
4.8
4.6
4.4
4.2
4.0
-4
-3
-2
-1
0
1
2
3
4
Yaw Angle - deg.

Fig. 18

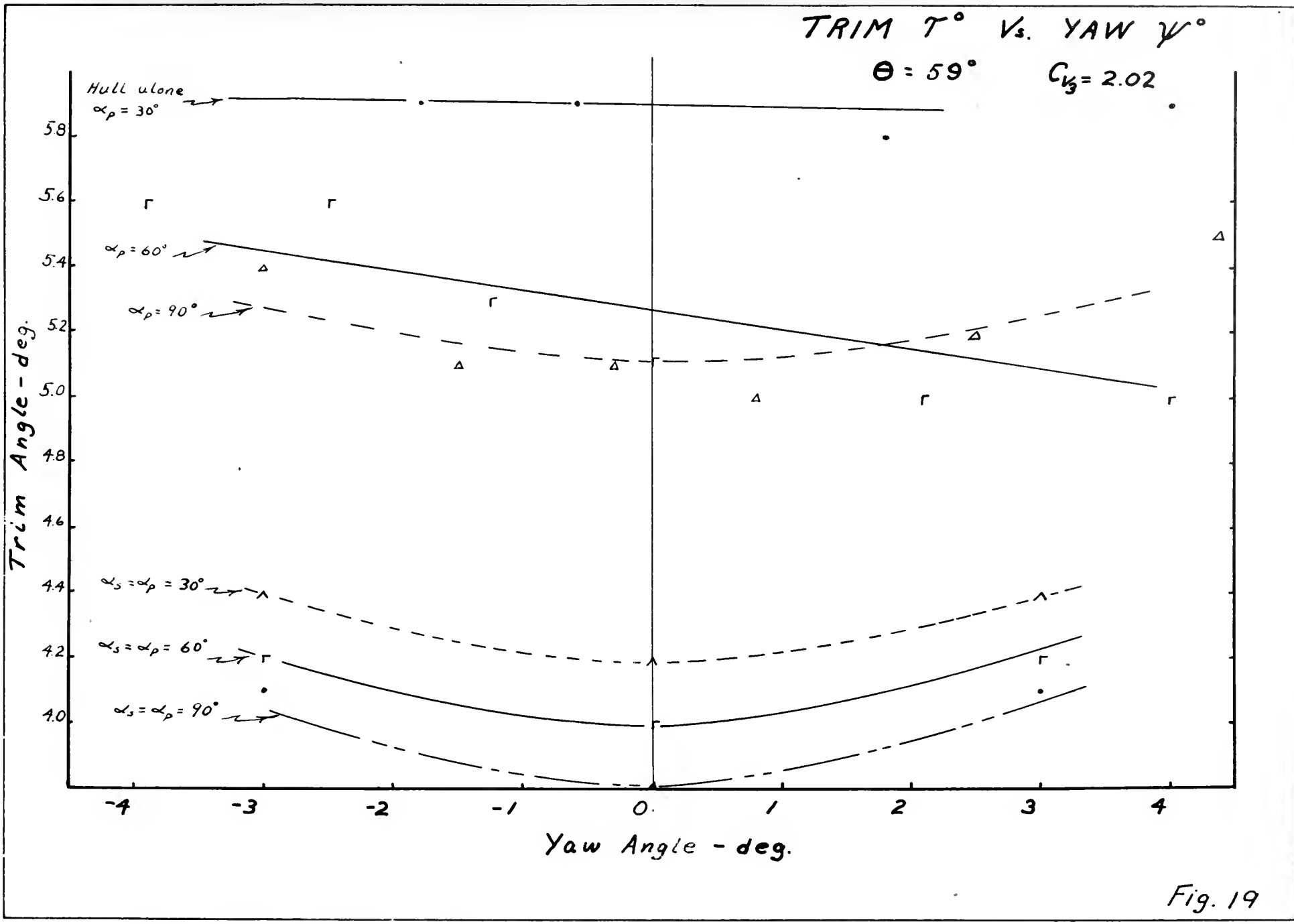
TRIM T° Vs. YAW Ψ°
Θ = 59°
C_{V_3} = 2.02
Hull alone
α_p = 30°
α_p = 60°
α_p = 90°
$\alpha_s = \alpha_p$ = 30°
$\alpha_s = \alpha_p$ = 60°
$\alpha_s = \alpha_p$ = 90°
Trim Angle - deg.
5.8
5.6
5.4
5.2
5.0
4.8
4.6
4.4
4.2
4.0
-4
-3
-2
-1
0
1
2
3
4
Yaw Angle - deg.

Fig. 19

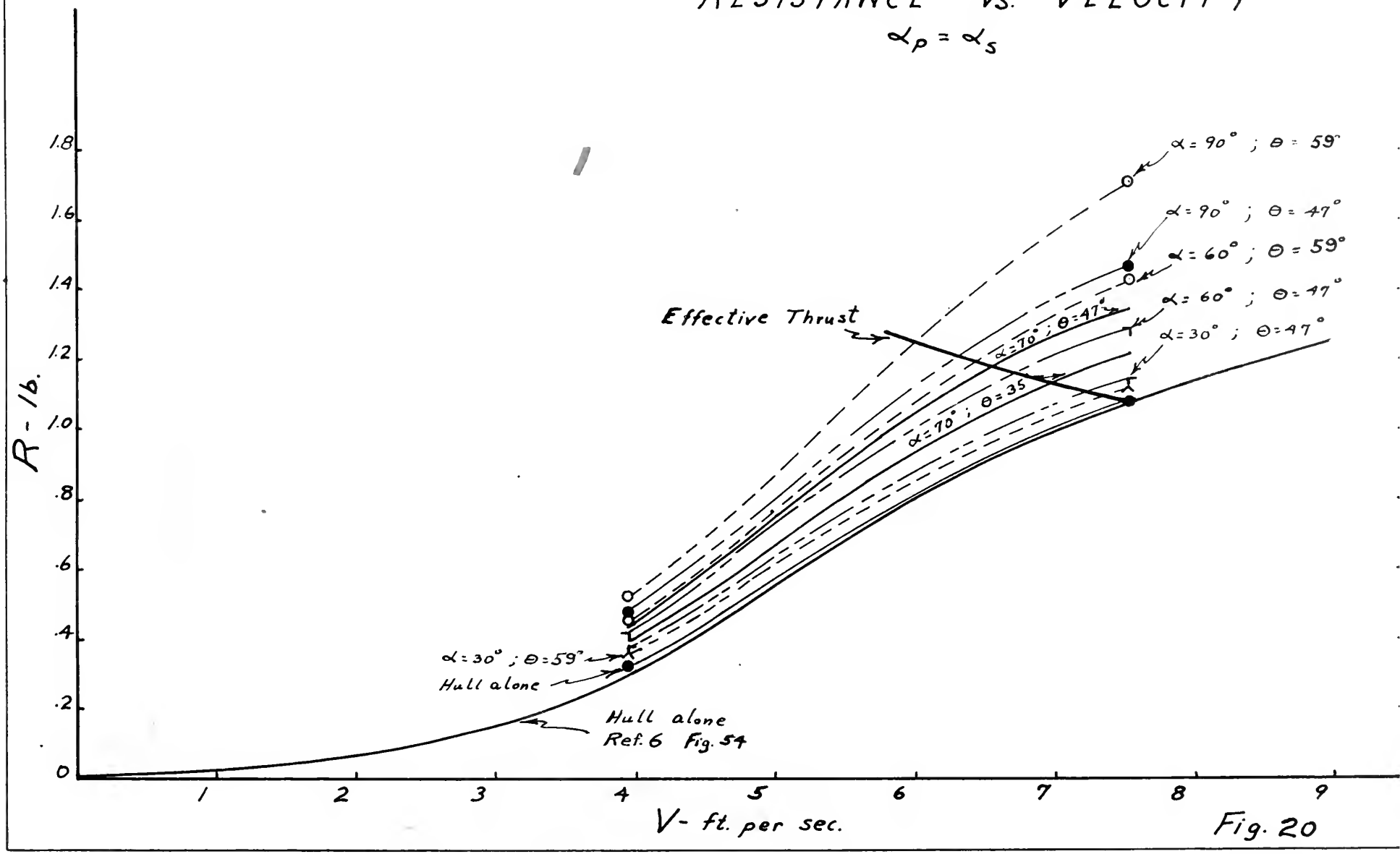
RESISTANCE Vs. VELOCITY
$\alpha_p = \alpha_s$
R - lb.
V - ft. per sec.
1.8
1.6
1.4
1.2
1.0
.8
.6
.4
.2
0
1
2
3
4
5
6
7
8
9
Effective Thrust
$\alpha = 90°$; $\theta = 59°$
$\alpha = 90°$; $\theta = 47°$
$\alpha = 60°$; $\theta = 59°$
$\alpha = 60°$; $\theta = 47°$
$\alpha = 30°$; $\theta = 47°$
$\alpha = 70°$; $\theta = 47°$
$\alpha = 70°$; $\theta = 35$
$\alpha = 30°$; $\theta = 59°$
Hull alone
Hull alone
Ref. 6 Fig. 54

Fig. 20

$\frac{R}{V^2}$ Vs α

$$C_D = \frac{R}{\frac{1}{2}\rho V^2 A}$$

A = constant

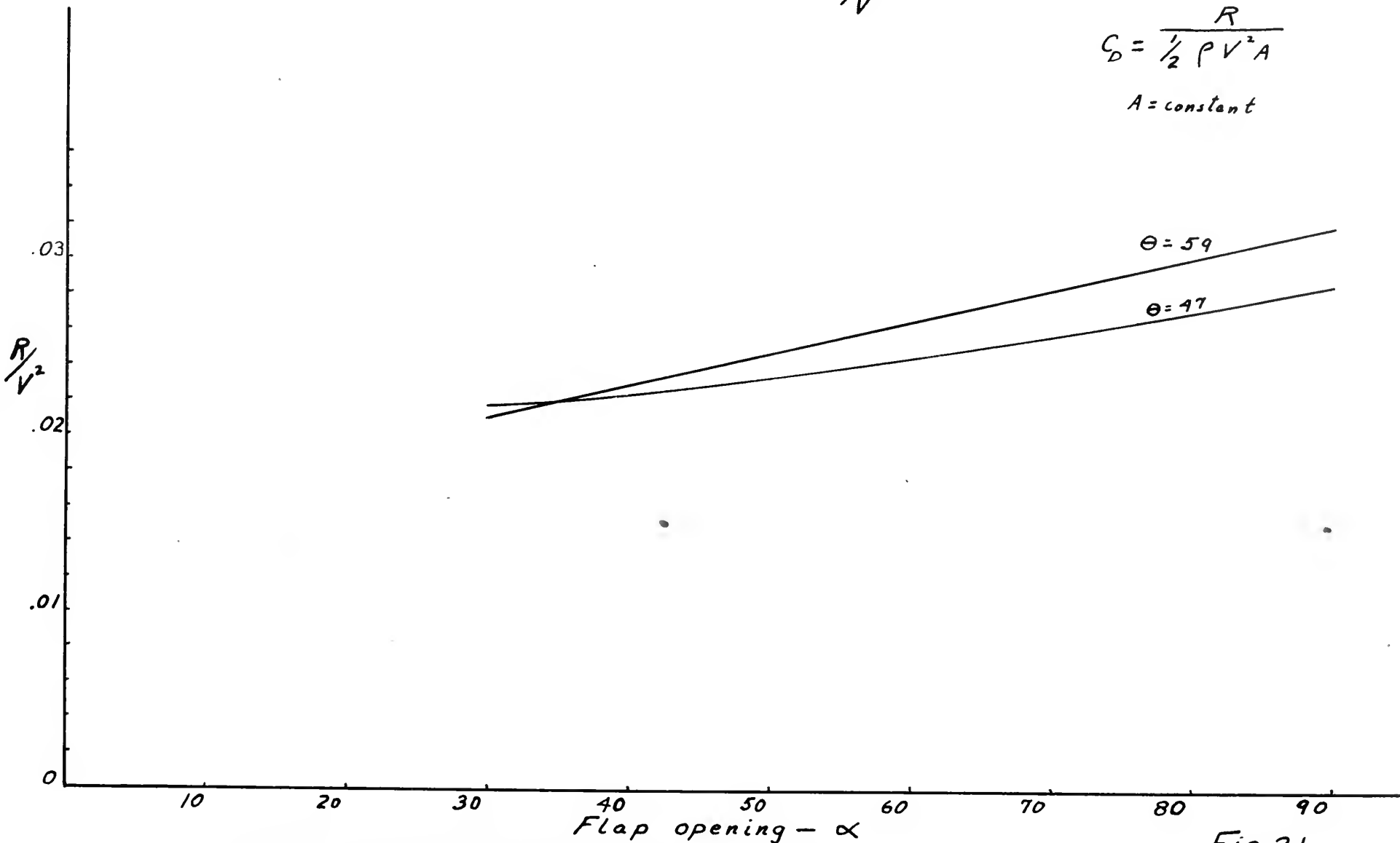

Fig. 21

STATIC PITCHING MOMENT CURVES

C_M Vs. α - deg.

$\Theta = 47^\circ$ α_p alone

$C_{V_1} = 1.06$

$C_{V_2} = 1.54$

$C_{V_3} = 2.02$

$C_M = \frac{M}{\frac{\rho}{2} V^2 A L}$

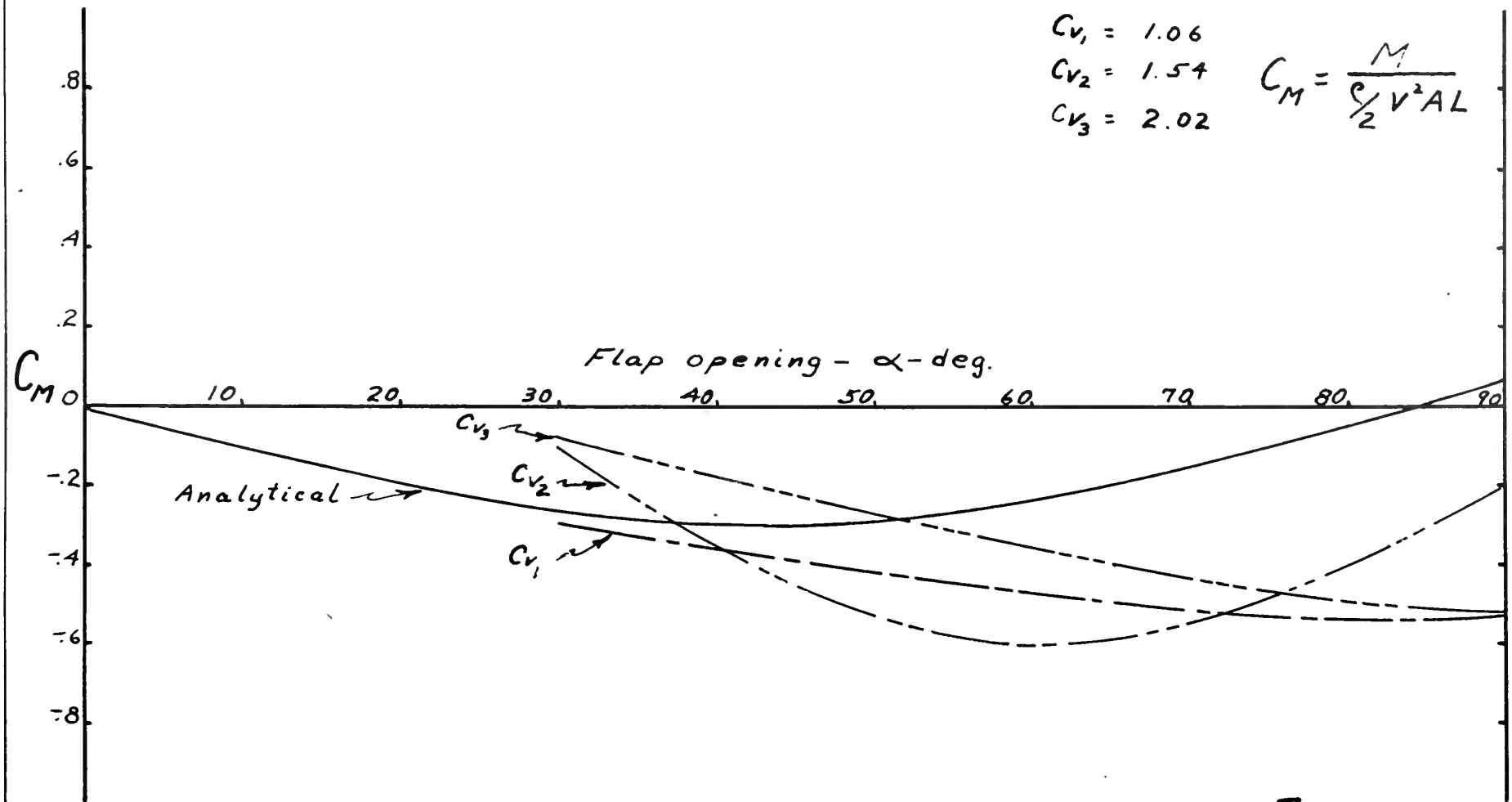

Fig. 23

STATIC PITCHING MOMENT CURVES

C_M Vs. α - deg.

$\theta = 59°$ α_p alone

$C_{V_1} = 1.06$

$C_{V_2} = 1.54$

$C_{V_3} = 2.02$

$$C_M = \frac{M}{\rho/2 V^2 A L}$$

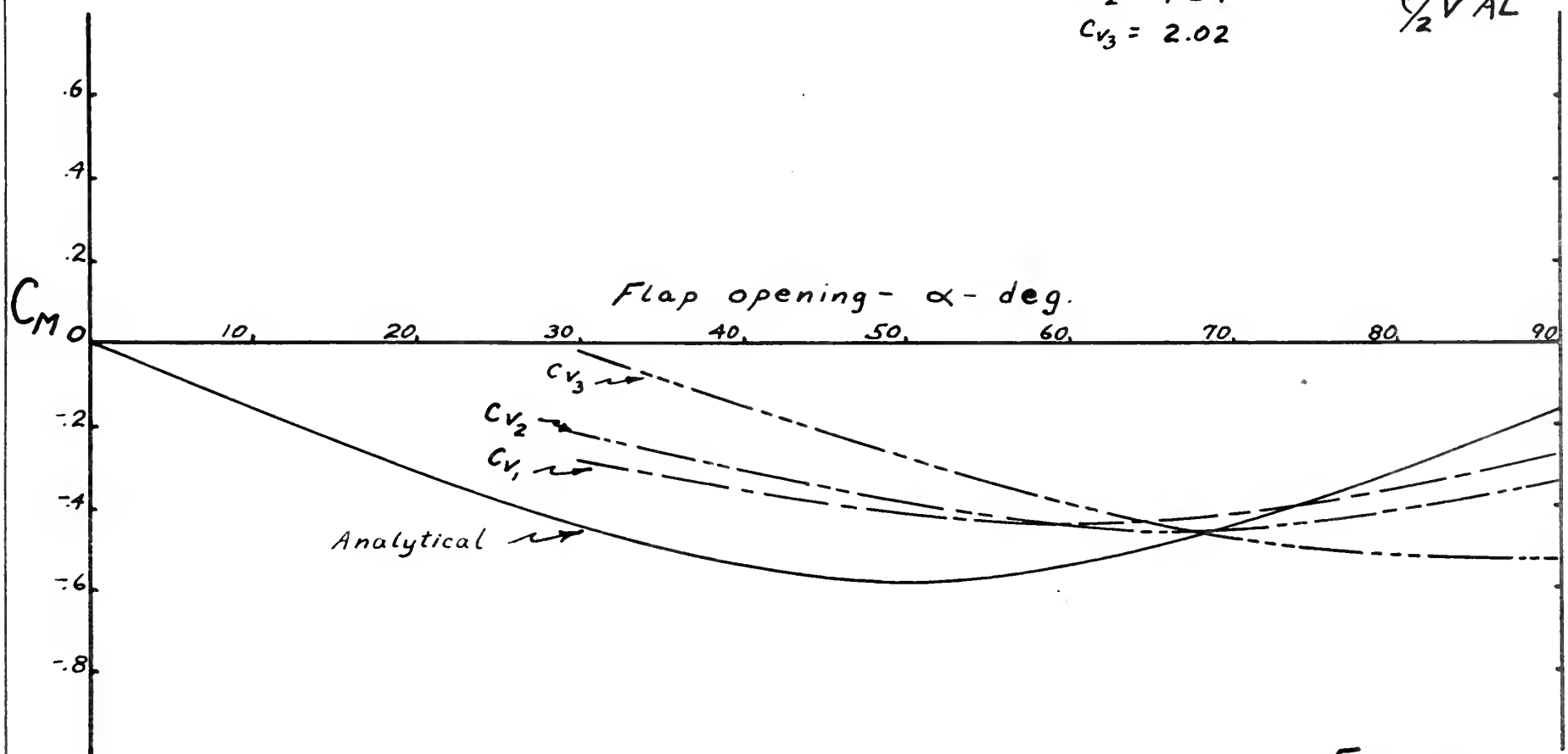

Fig. 24

STATIC PITCHING MOMENT CURVES

C_M Vs. α - deg.

$\Theta = 21°$ $\qquad \alpha_p = \alpha_s$

$C_{V_1} = 1.06$
$C_{V_2} = 1.54$
$C_{V_3} = 2.02$

$$C_M = \frac{M}{\frac{\rho}{2} V^2 A L}$$

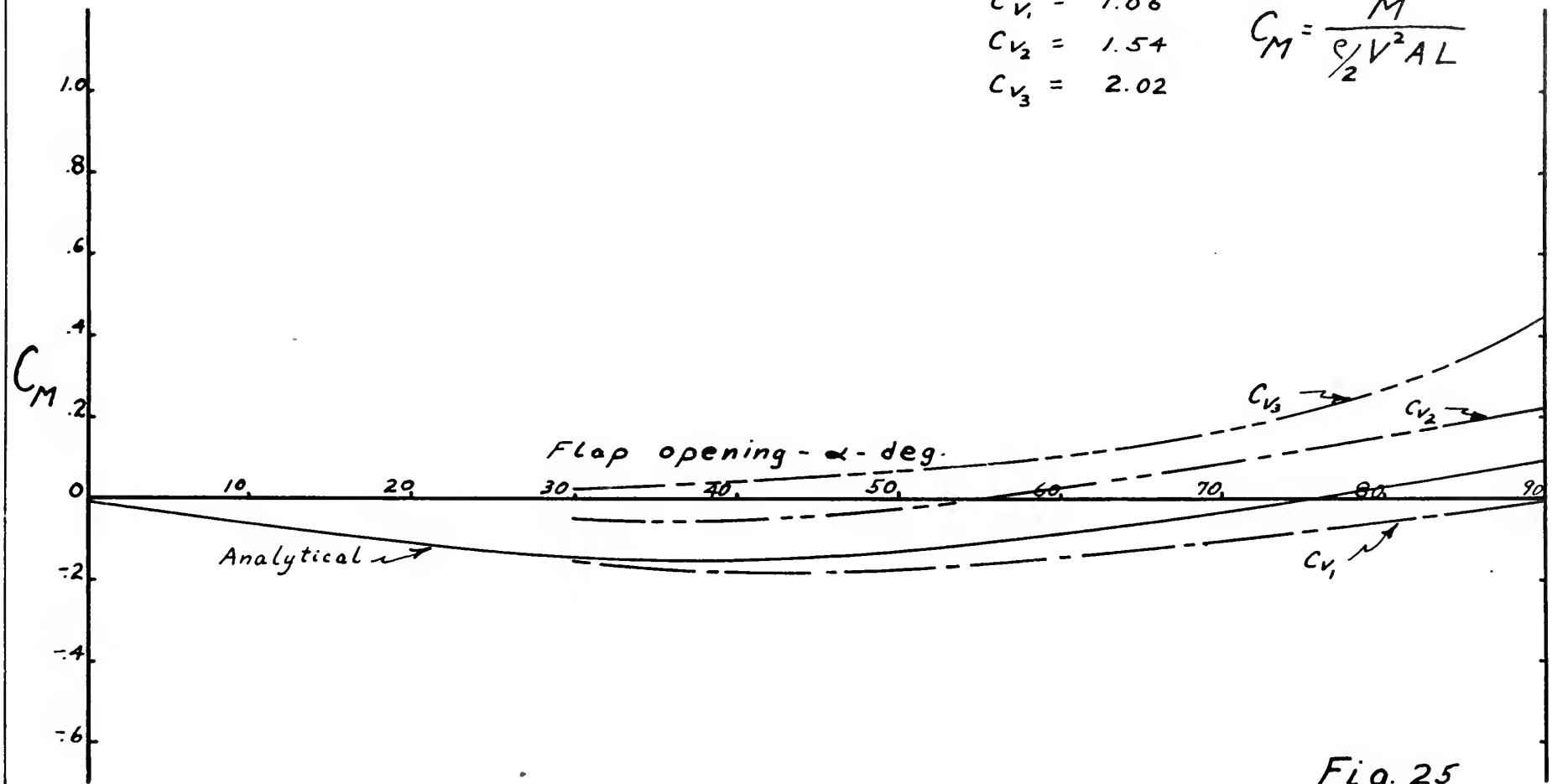

Fig. 25

STATIC PITCHING MOMENT CURVES

C_M Vs. α - deg.

$\Theta = 47°$ $\qquad \alpha_p = \alpha_s$

$C_{V_1} = 1.06$

$C_{V_2} = 1.54$

$C_{V_3} = 2.02$

$$C_M = \frac{M}{\rho/2 \, V^2 A L}$$

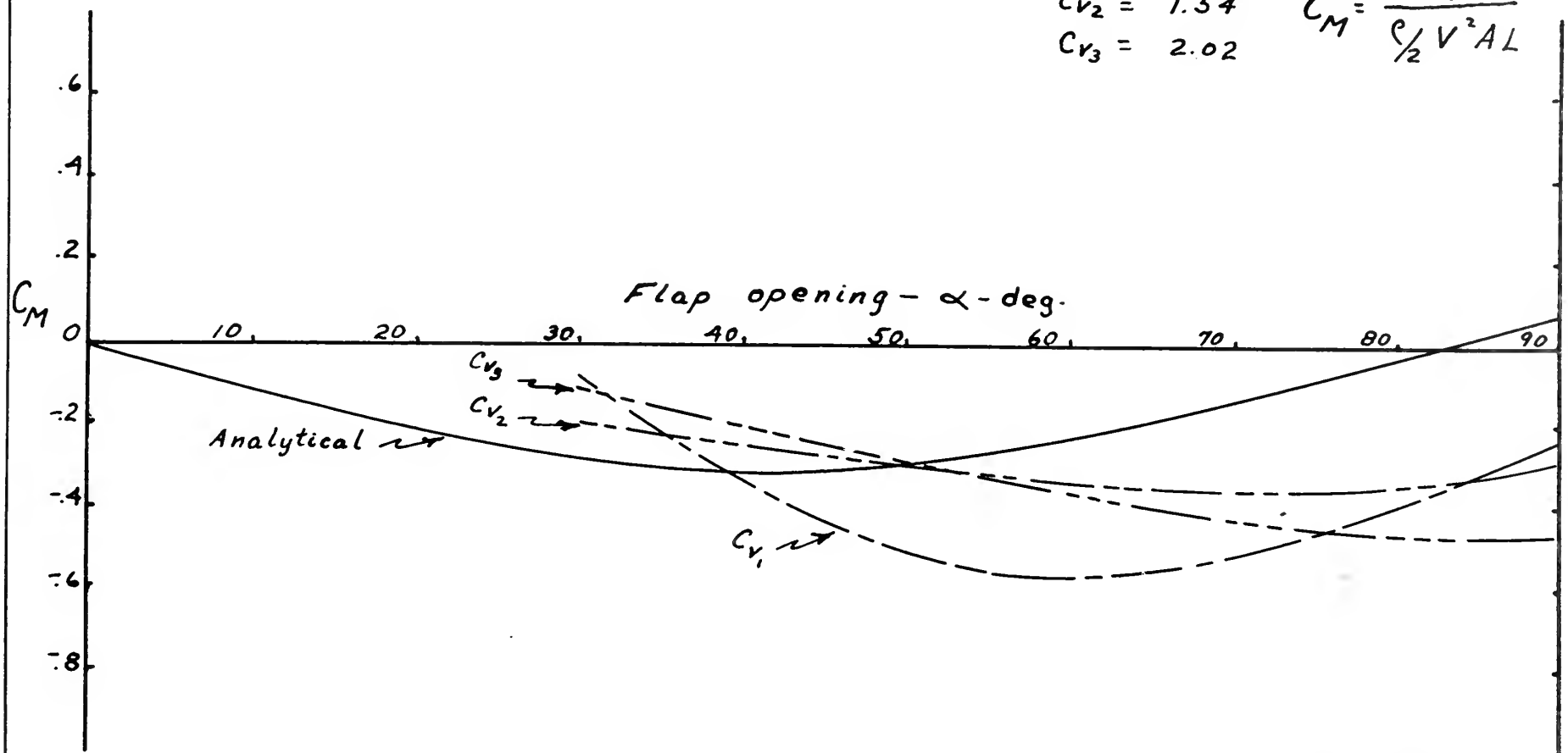

Fig. 26

STATIC PITCHING MOMENT CURVES

C_M Vs. α. deg

$\theta = 59°$ $\quad \alpha_p = \alpha_s$

$C_{V_1} = 1.06$

$C_{V_2} = 1.54$

$C_{V_3} = 2.02$

$$C_M = \frac{M}{\rho/2 \, V^2 AL}$$

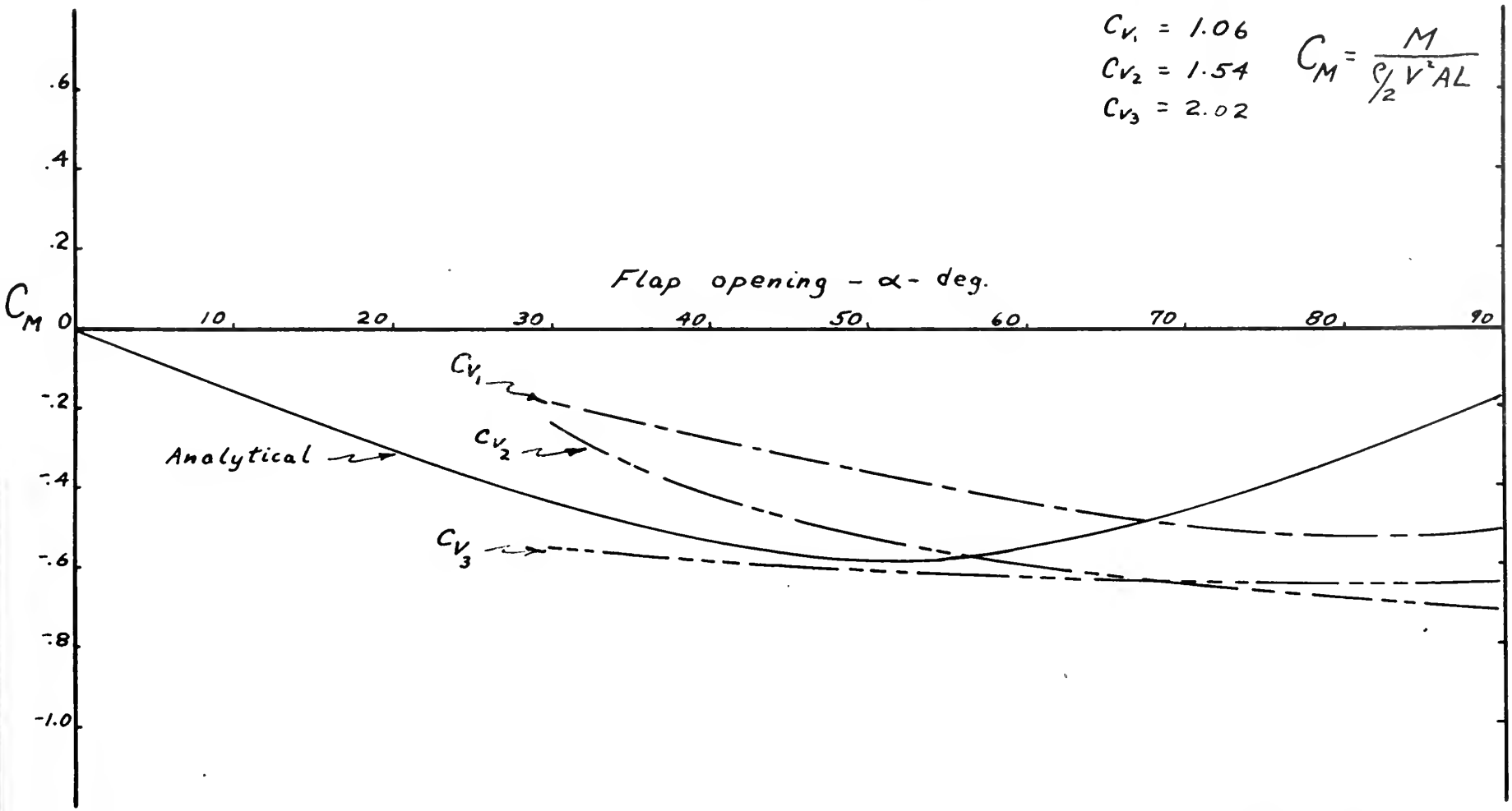

Fig. 27

STATIC PITCHING MOMENT CURVES

Analytical equation

$\beta = 20°$

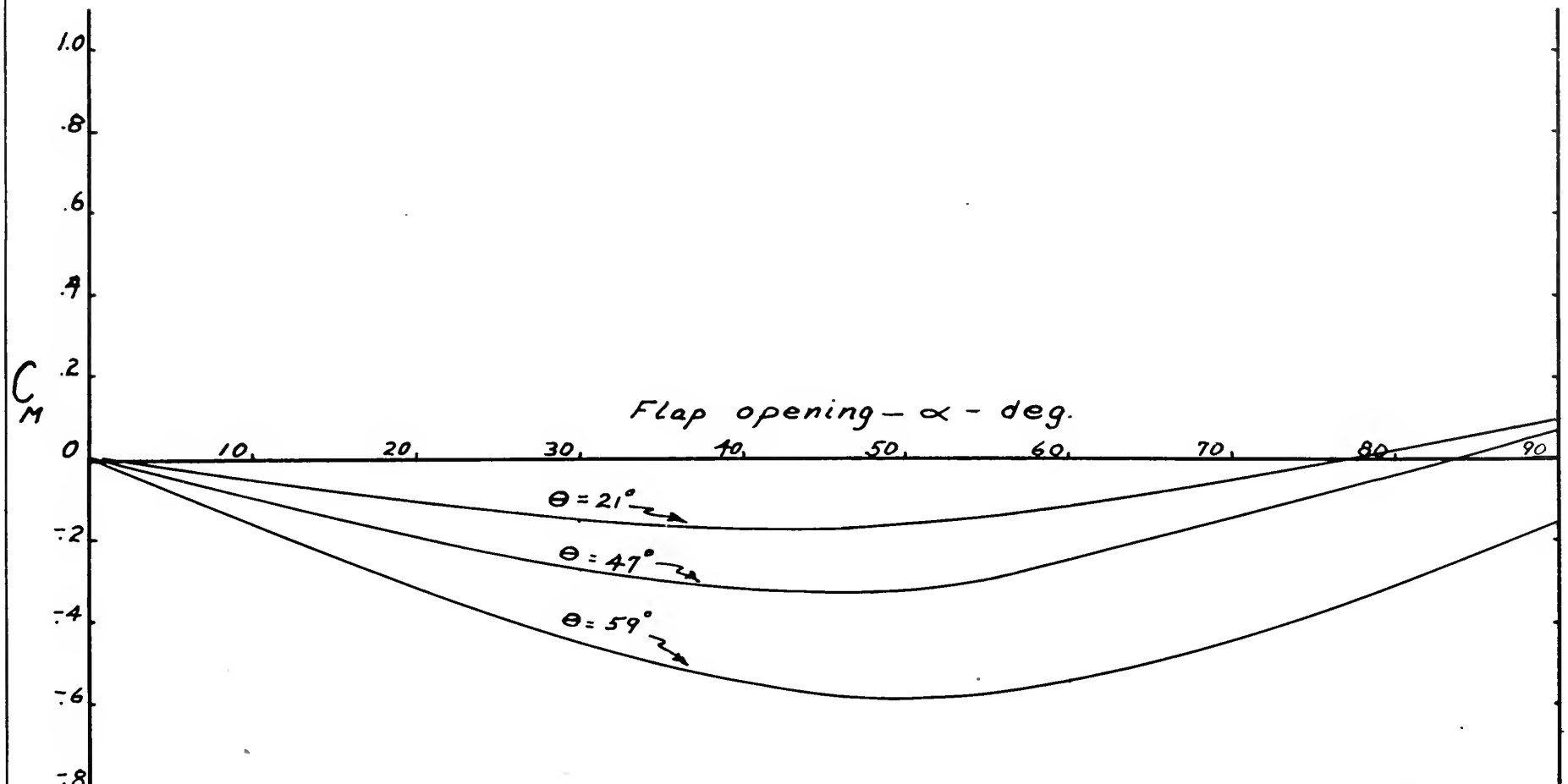

Fig. 28

STATIC PITCHING MOMENT CURVES

Analytical equation

$\beta = 40°$

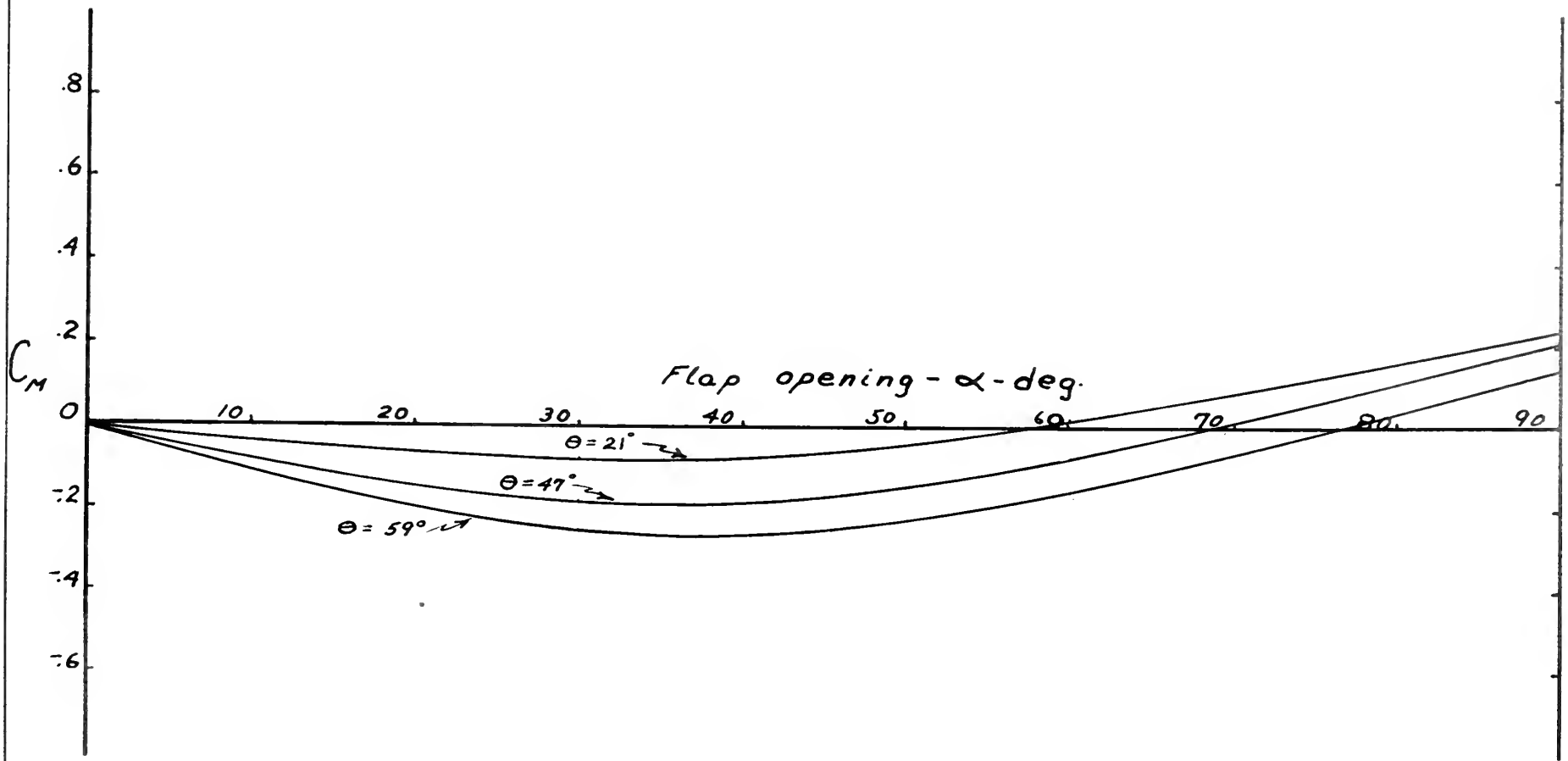

Fig. 29

$\frac{1}{F}$ Vs. V

$\frac{V}{F}$ Vs. V

Landing Run Time $T = \frac{W}{g}\int \frac{1}{F}\,dV$

Landing Run Distance $S = \frac{W}{g}\int \frac{V}{F}\,dV$

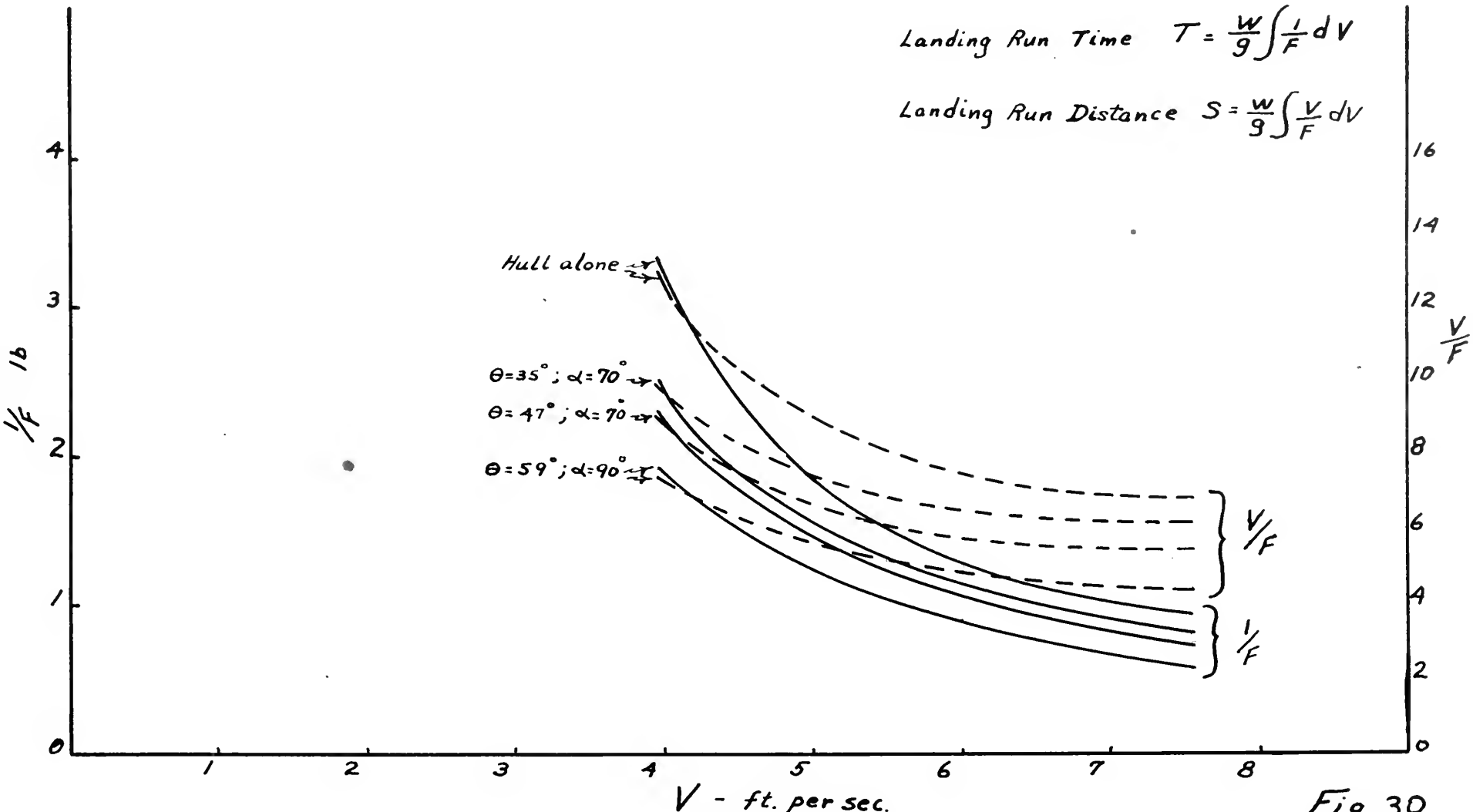

Fig. 30

GEOMETRY OF HYDROFLAP FOR THE ANALYTICAL SOLUTION.

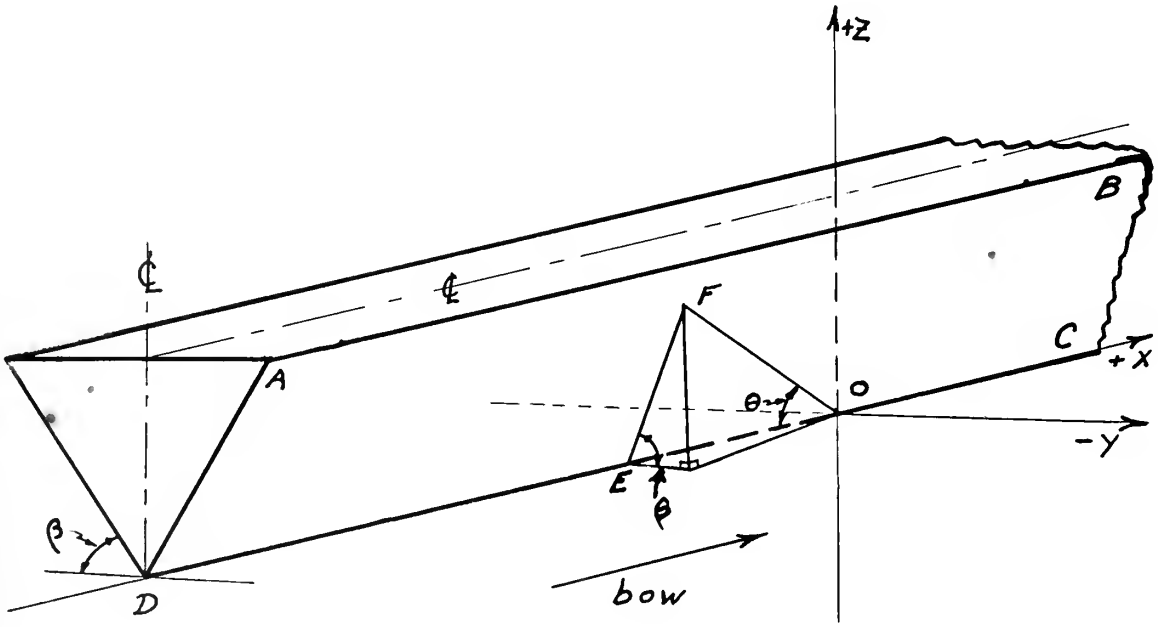

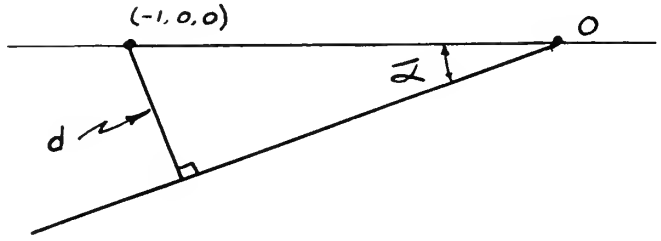

Fig. 31